GROWTH OF GOLD FILMS ON QUARTZ SURFACES FOR QUARTZ CRYSTAL MICROBALANCE APPLICATION

A THESIS SUBMITTED TO
THE GRADUATE SCHOOL OF NATURAL AND APPLIED SCIENCES
OF
MIDDLE EAST TECHNICAL UNIVERSITY

BY

BERRİN ÖZKAN

IN PARTIAL FULFILLMENT OF THE REQUIREMENTS
FOR
THE DEGREE OF MASTER OF SCIENCE
IN
CHEMISTRY

JULY 2010

Approval of the thesis:

GROWTH OF GOLD FILMS ON QUARTZ SURFACES FOR QUARTZ CRYSTAL MICROBALANCE APPLICATION

submitted by **BERRİN ÖZKAN** in partial fulfillment of the requirements for the degree of **Master of Science in Chemistry Department, Middle East Technical University** by,

Prof. Dr. Canan ÖZGEN _____
Dean, Graduate School of **Natural and Applied Sciences**

Prof. Dr. İlker ÖZKAN _____
Head of Department, **Chemistry**

Assist. Prof. Dr. Mehmet Fatih DANIŞMAN _____
Supervisor, **Chemistry Department, METU**

Examining Comitee Members:

Prof. Dr. Osman Yavuz ATAMAN _____
Chemistry Dept., METU

Assist. Prof. Dr. Mehmet Fatih DANIŞMAN _____
Chemistry Dept., METU

Prof. Dr. Mehmet PARLAK _____
Physics Dept., METU

Prof. Dr. Erdal BAYRAMLI _____
Chemistry Dept., METU

Assist. Prof. Dr. Okan ESENTÜRK _____
Chemistry Dept., METU

Date: 16 July 2010

.

I hereby declare that all information in this document has been obtained and presented in accordance with academic rules and ethical conduct. I also declare that, as required by these rules and conduct, I have fully cited and referenced all materials and results that are not original to this work.

Name, Lastname: Berrin Özkan

Signature:

ABSTRACT

GROWTH OF GOLD FILMS ON QUARTZ SURFACES FOR QUARTZ CRYSTAL MICROBALANCE APPLICATION

Özkan, Berrin

M. Sc., Department of Chemistry

Supervisor: Assist. Prof. Dr. Mehmet Fatih Danışman

July 2010, 57 pages

In this study, we have investigated the effect of substrate temperature, use of adhesive layer, deposition rate, annealing and substrate prebaking on the morphology of gold films deposited onto quartz surfaces. For the film growth, physical vapor deposition methods namely electron beam and thermal depositions have been used. Surface morphology of the films have been characterized with atomic force microscopy. Our aim was to confirm the general trends observed for these parameters in our evaporator system for a limited working range in order to produce gold films which are suitable to be used simultaneously for quartz crystal microbalance and helium atom diffraction measurements.

At the end of this study, we confirmed the general trends regarding the effect of these parameters stated in literature except annealing process. We obtained a minimum 170 nm^2 atomically flat surface with a roughness value smaller than 0.200 nm by thermal deposition method.

Keywords: Gold Film Growth on Quartz Surface, Quartz Crystal Microbalance, Atomic Force Microscopy.

ÖZ

KUVARS KRİSTAL MİKROTERAZİ UYGULAMALARI İÇİN KUVARS YÜZEYLER ÜZERİNDE ALTIN FİLMLERİN BÜYÜTÜLMESİ

Özkan, Berrin

Yüksek Lisans, Kimya Bölümü

Tez Yöneticisi: Yard. Doç. Dr. Mehmet Fatih Danışman

Temmuz 2010, 57 sayfa

Bu çalışmada, yüzey sıcaklığının, yapıştırıcı tabaka kullanımının, kaplama hızının, tavlamanın ve alttaşın kaplama öncesi ısıtılmasının, kuvars yüzeyler üzerinde büyütülen altın filmlerin morfolojisine olan etkileri araştırılmıştır. Filmlerin büyütülmesi için, fiziksel buhar kaplama metodları olan elektron demeti ve ısıl kaplama metodları kullanılmıştır. Filmlerin yüzey morfolojisi atomik kuvvet mikroskobu ile karakterize edilmiştir. Belirtilen parametrelerin etkilerine ilişkin genel eğilimlerin mevcut buharlaştırma sisteminde sınırlı bir çalışma aralığında doğrulanarak, aynı anda kuvars kristal mikro terazi ve helyum atomu difraksiyonu ölçümlerinde kullanılmaya uygun altın filmlerin büyütülmesi amaçlanmıştır.

Bu çalışmanın sonucunda, tavlama dışında tüm parametrelerin etkilerine ilişkin olarak literatürde belirtilmiş genel eğilimler doğrulanmıştır. Isısal kaplama metodu ile yüzey pürüzlülüğü 0.200 nm'den düşük, minimum 170 nm^2 alana sahip atomik seviyede düz alanlar elde edilmiştir.

Anahtar Kelimeler: Kuvars Yüzey Üzerinde Altın Film Büyütülmesi, Kuvars Kristal Mikro Terazi, Atomik Kuvvet Mikroskobu.

To my dear mother and father

ACKNOWLEDGEMENTS

I would like to express my appreciation to my supervisor Assist. Prof. Dr. Mehmet Fatih DANIŞMAN for his support and guidance throughout this study.

I would like to express my appreciation to Prof. Dr. Raşit TURAN for his support regarding use of evaporator system in his laboratory.

I would like to thank to Prof. Dr. Gülsün GÖKAĞAÇ for her support regarding use of AFM instrument in her laboratory.

I would like to thank to Mustafa KULAKÇI for his endless help regarding film deposition process.

I would like to thank to Dr. İbrahim ÇAM, Burkan KAPLAN, Hüseyin Avni VURAL and Fatih ŞEN for their help regarding AFM imaging.

I would like to thank to TÜBİTAK for funding this study.

I would like to thank to my dear friends Ebru ÜNEL, Feriye ŞENOL, Meryem KARABULUT, Tuğba ORHAN and Zafer ÖZTÜRK for their support during this challenging period.

Lastly, my deepest gratitude goes to my dear mother Birsen ÖZKAN and my dear father Ali ÖZKAN who always supported me.

TABLE OF CONTENTS

LIST OF FIGURES

LIST OF TABLES

CHAPTER 1

INTRODUCTION

Gold thin films, among the crystalline metal thin films, is the choice of substrate material for a wide range of academical research purposes and industrial applications [1-9]. The importance of gold originates from its characteristics. Due to having crystalline structure, almost inert character and high electrical conductivity, gold has a wide application range. Atomically flat gold substrates can be used in order to image adsorbate layers by using scanning probe microscopy techniques such as atomic force microscopy [10-12]. Besides, gold substrate is the subject of interest due to the formation of self-assembled monolayers (SAMs) on it via a covalent coordination between gold and sulfur of thiol group. These SAMs can be utilized for many different device applications such as biosensors and organic electronics [13-16]. Apart from these, gold is used in electronic devices [17-18]. In addition, it can be used as electrode surface for electrochemical purposes and quartz crystal microbalance applications [19-20].

In these applications, single crystalline gold substrates can be used. However, since it is highly expensive due to required special preparation procedures and possibility of contamination during handling, gold thin films are being used as an alternative substrate where single crystal surfaces are not required [5,9,21-27].

In this thesis study, our aim was to produce gold films on quartz surfaces that are suitable to be used simultaneously for quartz crystal microbalance and helium atom diffraction measurements.

1.1 Quartz Crystal Microbalance

Quartz crytal microbalance (QCM), as the name ''microbalance'' implies, is used for mass determination in thin film deposition process. Quartz is a piezoelectric material which means when electrical potential is applied to it, there occurs different motional modes due to change in orientation of dipoles in quartz depending on the crystal structure of it. Among these motional modes, shear motion which is the motion parallel to the quartz surface is the relevant one for the working mechanism of QCM and is observed for AT cut quartz crystals [19]. These type of quartz crystals are fabricated by cutting it with an angle (θ) of about $35^0 15'$ to the optic axis of it [28]. The schematic representation of an AT cut quartz crystal is shown in the figure 1.1.

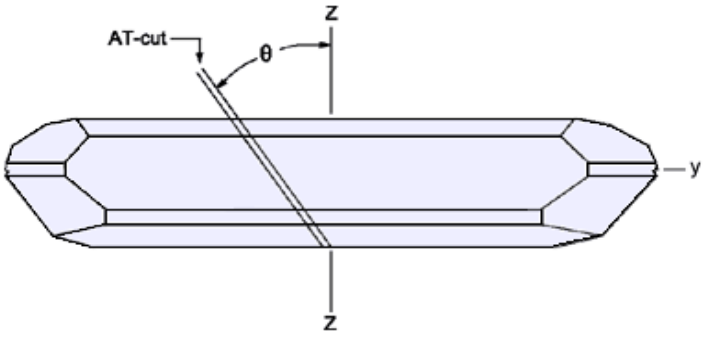

Figure 1.1. Schematic representation of an AT cut quartz crystal. Figure is reproduced from ref. 29.

The figure 1.2 shows how an applied electrical potential causes a change in orientation of dipoles and a shear motion in an AT cut quartz crystal surface.

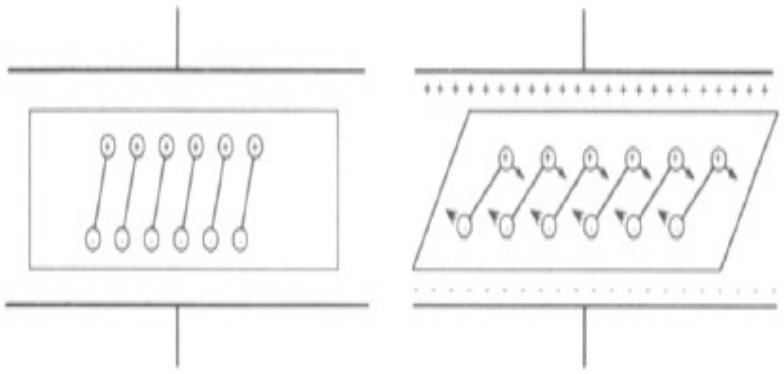

Figure 1.2. Reorientation of dipoles in an AT cut quartz crystal due to the applied electrical field. Figure is reproduced from ref. 19.

In the presence of electrical field, quartz crystal undergoes a vibrational motion and this causes an acoustic wave propagating through the quartz crystal. When the wavelength of this wave is equal to two times of the thickness of the quartz crystal, this propagating wave becomes a standing wave and its frequency is called resonance frequency [19].

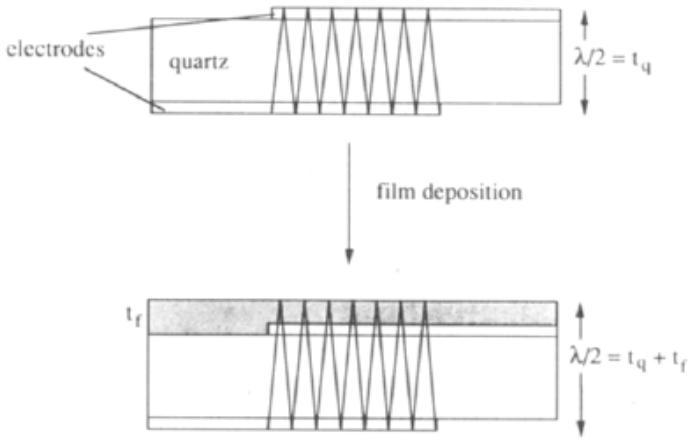

Figure 1.3. Schematic representation of the shear wave depending on the thickness. Figure is reproduced from ref. 19.

As it is shown in figure 1.3, during film deposition on quartz surface, thickness changes and this causes a change in resonance frequency. By measuring the resonance frequency shift, one can determine the deposited mass according to the following equation:

$$\Delta f = -\frac{2 f_{res}^2}{n Z_q} \frac{m}{A} \qquad (1.1)$$

where f_{res} is the resonance frequency of quartz crystal, m is the mass of the adsorbed material, A is the area of the electrodes, Z_q is the acoustic impedance of quartz and n is the order of resonance [19]. By using a secondary method in order to determine the thickness of the deposited film, mass can be used as a measure of thickness.

The working mechanism of QCM requires applying electrical potential to the quartz and measuring its resonance frequency shift. For this reason, gold films

are deposited on both sides of quartz. The properties of these films have an important role in determining the working efficiency of QCM [19].

In vacuum, there are two important necessities that the gold electrode should satisfy for an accurate frequency shift measurement in a QCM study.

1) The deposited gold film should be rigid on quartz surface so that quartz and gold film can behave as a ''composite resonator'' whose thickness is equal to the sum of quartz crystal and gold electrode thicknesses [19,30].

2) The deposited gold film should be macroscopically uniform; i.e. it should have a uniform thickness value in all electrode region on the quartz surface in order to observe a uniform mass distribution; i.e. a uniform thickness value during deposition [19].

According to the first necessity, the deposited gold film should be strongly adsorbed to the quartz surface. It should be mechanically stable enough to attach the electrical connectors on the gold electrode surfaces and to mount the quartz crystal on the sample holder of the deposition system without giving any damage to the gold surfaces. And according to the second condition, the deposition should be macroscopically homogeneous in order to obtain a homogeneous thickness value and consequently, to measure a nearly accurate resonance frequency shift.

Besides these, in our study additional film properties are needed since our aim is to use this gold deposited quartz simultaneously as the substrate for both QCM and helium atom diffraction measurements.

1.2 Helium Atom Diffraction

Helium atom diffraction is used to determine the surface crystal structure of materials in a nondestructive way [30,31]. In order to obtain a reasonable diffraction pattern, diffraction peak intensities should be high and diffraction peak widths should be small. There are several factors affecting the peak intensity and peak width. Some of them are related to the instrument and others depend on the various surface properties of the sample. Among these properties, our subject of interest is the topography of the surface. In accordance with this limitation, high diffraction peak intensity for a particular crystal structure depends on the number of repetitive unit cells. High number of unit cells increases the peak intensity. On the other hand, small peak width depends on both number of unit cell and surface corrugation of the sample which is measure of the vertical deviations in the texture of surface. Small surface corrugation and again high number of unit cell decrease the diffraction peak width [30,32].

In the figure 1.4, the indicated results belong to morphologically two different gold films deposited on quartz surface. The deflection atomic force microscopy images and the related specular reflection intensities which have been obtained by helium atom diffraction are shown. The gold film in figure 1.4a has been purchased from a crystal manufacturer. It has been deposited on a 50 Å chromium layer with a rate of 10 Å/s, at 125 ^{0}C substrate temperature and at 10^{-5} torr background pressure. The one in figure 1.4b has been deposited onto bare quartz surface by Danışman; it has been evaporated with a rate of 0.2-0.3 Å/s, at 250 ^{0}C substrate temperature and at 10^{-5} torr background pressure [30].

As the domain size increases as it is shown in figure 1.4b, specular reflection peak intensity increases due to the increased number of unit cell and the peak width decreases again due to high number of unit cell although there is a considerable surface corrugation [30].

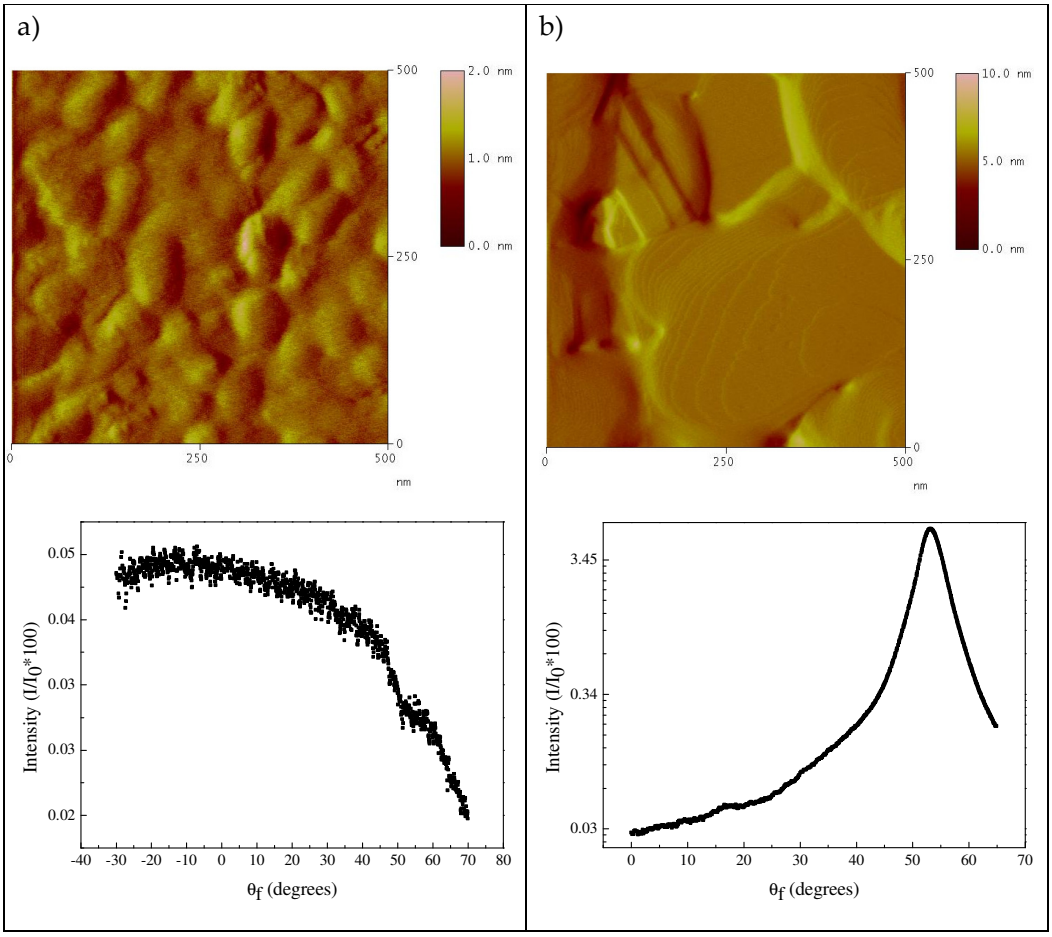

Figure 1.4. Deflection AFM images and helium atom scattering from a) the purchased gold film, b) the gold film deposited onto bare quartz surface by Danışman. The angle of incidence is 60^0 for helium atom diffraction. Figure is reproduced from ref. 30.

According to these diffraction results, in order to study with helium atom diffraction, gold films which are deposited on quartz surface should have large atomically flat regions which is a measure of large domain size; i.e. high number of unit cells, and small roughness value which is measure of small surface corrugation.

Ultimately, in this thesis study, it has been aimed to produce gold thin films which have

1) mechanical stability,
2) macroscopic homogeneity,
3) large atomically flat regions,
4) small roughness value.

1.3 Growth of Gold Thin Films

The desired gold films, with a thickness ranging from a nanometer to several micrometers, can be prepared in vacuum by means of physical deposition methods [5,6,9,15,16,20,22-24].

1.3.1. Physical Deposition Methods

Physical deposition methods basically aim to transfer the source material to the substrate surface without any composition change. Most of them can be classified under the title of physical vapor deposition methods. Physical vapor deposition methods include thin film deposition by means of vapor condensation of the source material onto the substrate surface. In evaporation method, the simplest way to form thin film, thermal energy is supplied to the source material which can be in solid or liquid phase in order to transform it to the vapor phase. This vapor expands into the vacuum chamber and condenses onto the substrate surface with lower temperature than that of source material [31,33].

In this thesis study, the evaporation process has been achieved by electrical heating and high-energy electron bombardment. In the former method, electric

current is passed through the sample holder containing the source material and in the latter, high-energy electrons are directed through the surface of source material in order to achieve vaporization [31,33].

1.3.2. Growth Modes

During deposition process, according to the substrate-adsorbate and adsorbate-adsorbate interactions, three different growth modes can be observed. These are named as Volmer-Weber (island growth), Frank-van der Merwe (layer by layer growth) and Stranski-Krastanov (layer plus island growth) growth modes; these are shown in figure 1.5 [31,33].

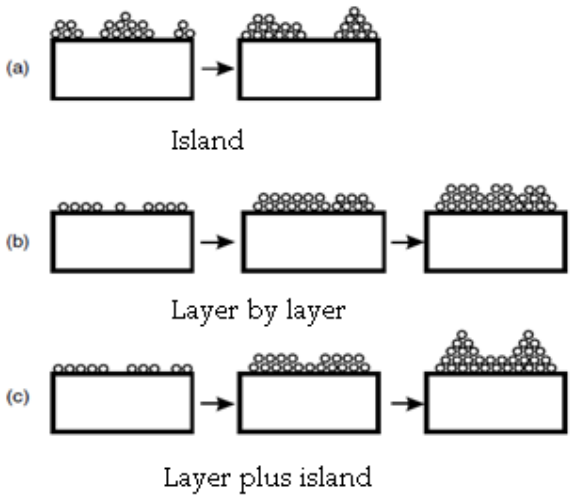

Figure 1.5. Growth modes observed in thin film formation; (a) Volmer-Weber, (b) Frank-van der Merwe, (c) Stranski-Krastanov. Figure is reproduced from ref 33.

Film morphology depends mostly on the growth mode, which is determined by the nature of substrate, adsorbate, and the deposition parameters which are optimized by taking growth mode into consideration [31,33].

1.3.3. Deposition Parameters

The main deposition parameters affecting film morphology are substrate temperature, deposition rate and film thickness [31,33]. In addition to these, use of adhesive layer and annealing of film and substrate are the two factors which have important role in film morphology [1,24,25,26,34,35]. In order to obtain the desired film properties, all of these are optimized on the thermodynamic basis of film growth according to the nature of adsorbate and substrate [31,33].

From the perspective of the substrate type, in literature, most of the studies regarding gold film growth and its morphological analysis have focused on the use of silicon and especially mica as the substrate material [14,21,24,26,27,35,36,37]. Silicon substrates have been used for electronic applications [35]. Mica has been the subject of interest since it has very small surface corrugation, it is cheap and convenient for contamination free usage thanks to easy cleavage [21,35]. Quartz has not been preferred generally since it has a rough surface and it is not suitable for gold to adsorb on it strongly. On the other hand, it has been concluded from the studies where quartz has been the substrate material that in necessary applications adhesive layer can be used, such as chromium and titanium layer, in order to increase the mechanic stability of the deposited gold films [26,34].

As for the deposition parameters, substrate temperature, deposition rate and film thickness has been mostly emphasized parameters in the literature [1,3,5,7,9,21,23-27,36-38]. Especially, substrate temperature and deposition rate have attracted

much interest since they have a direct effect on the film morphology by manipulating the growth mode. They have important role in manipulating the adhesion and diffusion processes. However, effect of film thickness has not been studied much since film thickness affects the morphology indirectly depending on the growth mode. Additionally, annealing of the substrate or the gold film has been utilized in order to have a gold film with smaller surface corrugation and larger grain size. Especially, flame annealing has been used for the gold films since it requires simple and cheap apparatus, and it is not time consuming. In their study, Nogues and Wanunu [21] have used flame-annealing in order to obtain gold films on mica with large atomically flat terraces. They have evaporated 100 nm thick gold film onto mica with a deposition rate of 0.5 Å/s without heating the substrate. Then, these films have been flame annealed under nitrogen atmosphere at 650 ^{0}C for 1 minute, at 480 ^{0}C for an additional minute and cooled down for 3 minutes by applying nitrogen gas stream. After flame-annealing, they have observed that grain size has increased and roughness value has decreased (figure 1.6). They have obtained atomically flat terraces with a size of 1 μm.

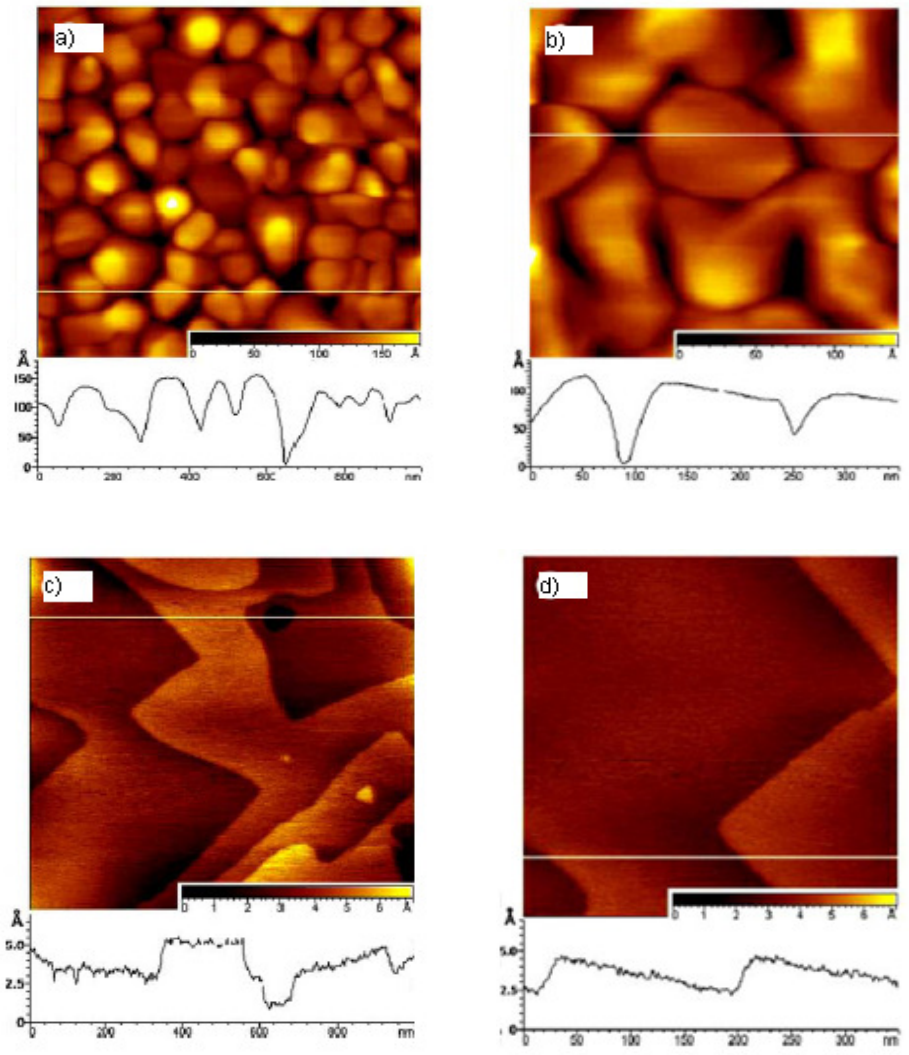

Figure 1.6. Tapping mode AFM images and line profiles of unannealed (a-b) and annealed (c-d) films. (a-c) represents for 1 μm x 1 μm scans and (b-d) represents for 0.35 μm x 0.35 μm scans. In line profiles, x scale represents the scan size; i.e. length of the scanned line. Figure is reproduced from ref. 21.

Lauer et al. [25] have also worked on the morphological healing of gold films deposited on glass by means of flame annealing. They used gold films on chromium-glass substrates with high nucleation density and flame annealed

these films at 850 ^{0}C for 10 minutes. As shown in the figure 1.7, tapping mode AFM images taken before and after flame annealing have proved that a considerable increase in grain size and atomically flat areas have been achieved by flame annealing process.

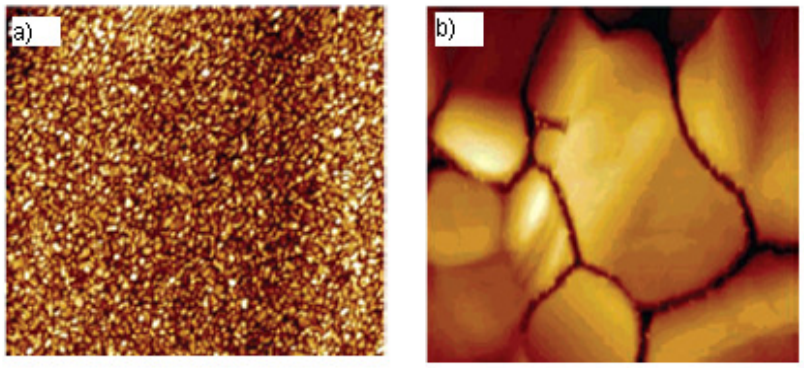

Figure 1.7. Tapping mode AFM height images of gold films before (a) and after (b) flame annealing for 1 μm x 1 μm scans. Figure is reproduced from ref. 25.

In another study, Dishner et al. [26] have studied the effect of substrate temperature at a deposition rate of 1 Å/s and again the effect of flame annealing for gold film on mica. At room temperature deposition, they have observed large number of small grains. On the other hand, they have reported that grain size has increased up to the substrate temperature of 380 ^{0}C. After this temperature, a very rough surface has been obtained. Besides, they have also stated that flame annealing has increased the grain size and resulted in regular flat grains with a surface area of 310 000 nm^2.

On the other side, Höpfner et al. [27] have tried to produce large monocystalline gold surfaces on mica by focusing on prebaking of mica, substrate temperature, deposition rate and annealing of deposited gold film. They have found that low substrate temperature resulted in amorphous film with small grain size. Then,

they have decided to deposite gold films at high temperature in order to increase the grain size. From a working range of substrate temperature, they have found 500 ^{0}C as the best value. And after prebaking of mica at 500 ^{0}C for 16 hours in order to remove surface contaminants, 150 nm gold film has been deposited with a rate of 1 nm/s at 500 ^{0}C. As it is shown in the figure 1.8, as the substrate temperature has increased, the grain size has also increased.

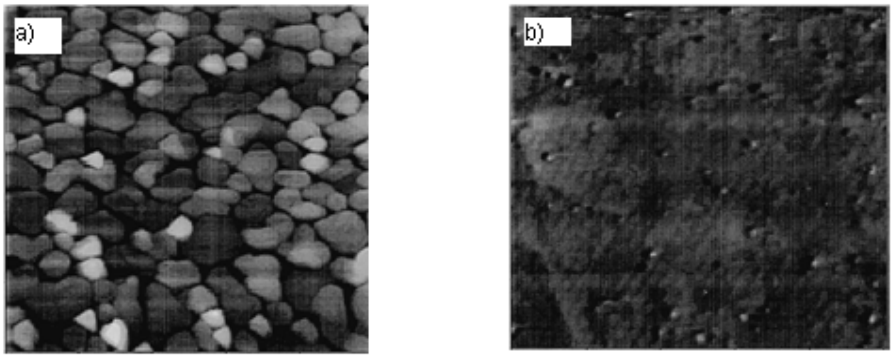

Figure 1.8. AFM images of gold film deposited on mica at room temperature (a) and at 500 ^{0}C (b) for 1 μm x 1 μm scans. Figure is reproduced from ref. 27.

Although large crystalline areas have been obtained at 500 ^{0}C, they have been observed to be separated by many deep holes. After that, another deposition has been carried out in two-step process again at the same temperature. The first 70 nm layer of the gold film has been deposited at a rate of 5 nm/s and the remaining 80 nm has been deposited at a much lower rate like 0.5 nm/s. By the high deposition rate applied in the first step, they have planned to eliminate the holes on the film via creating more nucleation sites. However, in this case, instead of holes, they have observed large crystalline areas with many spots (figure 1.9). Finally, all two films have been found as having large flat areas with an rms roughness value smaller than 1 nm. As an additional procedure, they have

applied flame annealing on these films, but they could not observe any positive effect on the film morphology.

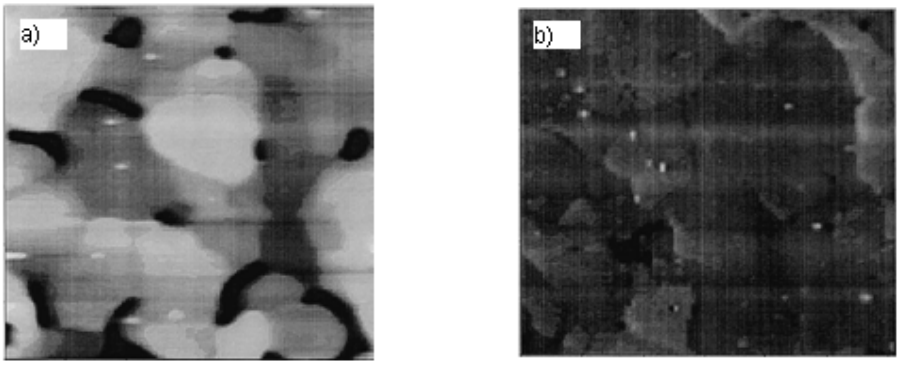

Figure 1.9. AFM images of gold film deposited on mica by single-step process (a) and by two-step process (b) for 3 μm x 3 μm scans. Figure is reproduced from ref. 27.

In another study, Hwang and Dubson [24] have investigated the morphological properties of gold films deposited on prebaked glass substrate at different thicknesses and substrate temperatures. All films have been deposited at a rate of 0.1 nm/s after prebaking of glass between 300-400 ^{0}C in vacuum for at least 12 hours. Film thickness has ranged from 20 to 80 nm and substrate temperature has ranged from 20 to 465 ^{0}C. They have observed that high substrate temperature and high film thickness resulted in larger average grain size. However, at high temperatures like 400 ^{0}C, they have observed large spots on atomically flat surfaces and at 300 ^{0}C, they have achieved to obtain 200x200 nm^2 atomically flat terraces with rms roughness of 0.03 nm although high substrate temperature has caused an increase in surface corrugation at large scale.

Again as for the effect of the substrate temperature, Higo et al. [37] have reported that high growth temperature increased the grain size of 150 nm gold film

deposited on mica. At 473 ^{0}C and with a deposition rate of 2.0 nm/s, they could have obtained smooth atomically flat surfaces with rms roughness of 0.78 nm for 10 μmx10 μm image (figure 1.10).

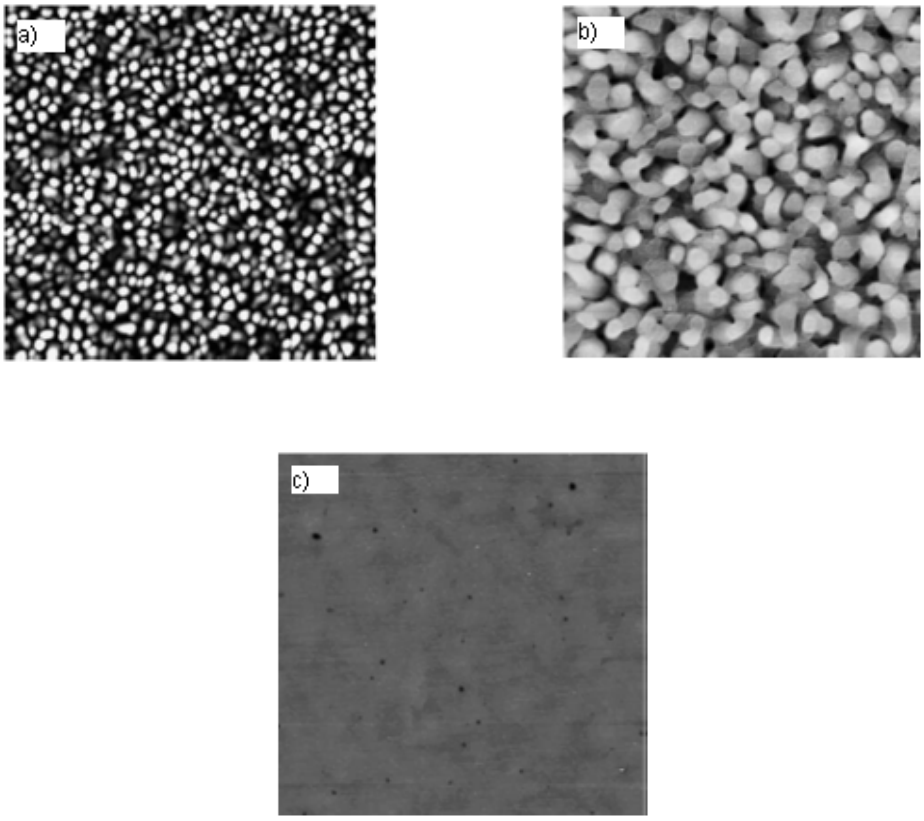

Figure 1.10. AFM images of gold film deposited on mica at room temperature (a) for 1 μm x 1 μm scan, at 260 ^{0}C (b) for 3 μm x 3 μm scan and at 473 ^{0}C (c) for 10 μm x 10 μm scan. Figure is reproduced from ref. 37.

From the literature studies, it has been concluded that the deposition parameters varies significantly depending on the apparatus. However, they indicate similar trends for the effect of these parameters on the film morphology. As the substrate temperature increases, the grain size increases, too [1,3,5,7,9,23,24,26,27,36,38]. Prebaking of the substrate surface before deposition is effective on removing

surface contaminants and eliminating the effect of contamination on the film morphology [24,27]. Annealing especially flame-annealing at a temperature higher than the substrate temperature decreases the surface corrugation and increases the grain size [21,25,26]. High deposition rate has been reported to cause an increase in the number of nucleation sites [27,37,38]. According to these results, in most studies, substrate temperature and deposition rate have been optimized so as to produce large atomically flat areas with small atomic corrugation.

In the light of these observations, we have deposited gold films onto the quartz surfaces taking into account the general trends observed for each deposition parameter. We have investigated the effect of these parameters in our evaporator system in order to produce films that are suitable to use simultaneously for QCM application and helium atom diffraction study. After deposition process, surface characterization of these films have been performed by atomic force microscopy.

CHAPTER 2

EXPERIMENTAL

In this chapter, the used materials will be introduced and a brief introduction about deposition and surface characterization methods will be given.

2.1 Materials

For this study, gold pellets with 99.999% purity and chromium pieces with 99.998% purity were purchased from Kurt J. Lesker Company in East Sussex, UK. AT cut quartz crystals were purchased from ICM Company in Oklahoma City, USA. Before deposition, quartz crystals have been cleaned with pure acetone and ethanol. Then, after drying with pure nitrogen gas, they have been used for film growth process. For atomic force microscopy analysis, doped silicon scanning probes were purchased from Nanosensors in Wetzlar, Germany.

2.2 Thermal and Electron Beam Deposition Methods

In this study, gold films and chromium films as adhesive layer were deposited onto AT cut quartz crystal surfaces by using thermal and electron beam deposition methods in the same evaporator. The evaporator apparatus have been constructed by Prof. Dr. Mehmet PARLAK and Mustafa KULAKÇI from Physics Department of Middle East Technical University. In thermal case,

vaporization has been achieved by passing electric current through the resistance-heated boat; a tungsten boat has been used for this purpose. Schematic representation of thermal evaporation system is shown in the figure 2.1.

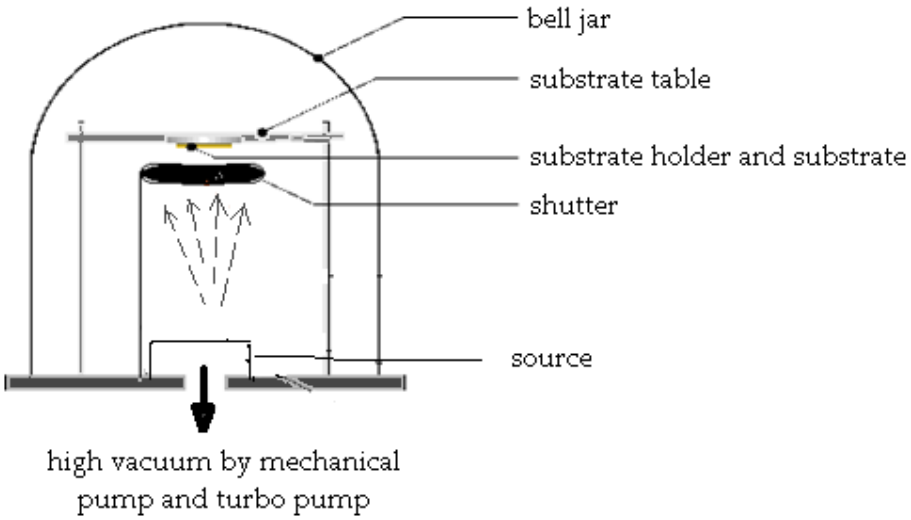

Figure 2.1. Schematic representation of thermal evaporation system. Figure is reproduced from ref. 39.

In electron beam deposition, vaporization has been achieved by sending intense beam of high-energy electrons to the source material as shown in the figure 2.2. Graphite crucible has been used in order to hold the source material.

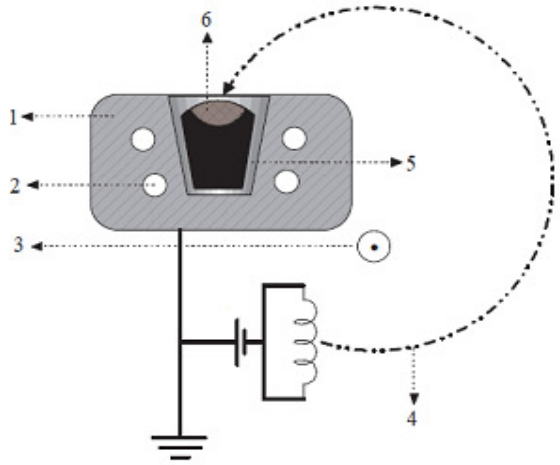

Figure 2.2. Schematic representation of electron beam evaporation system. 1) Hearth, 2) cooling water, 3) magnetic field, 4) focused electron beam, 5) source holder and 6) solid source material. Figure is reproduced from ref. 40.

As for the film growth process, sample holder has been fixed to 28 cm above the source and deposition has been started when the vacuum level of the evaporation system has dropped to about $4x10^{-6}$ torr. All depositions have been done at a vacuum level of about $6x10^{-6}$ torr. During deposition, cooling water has been passed through the source holder and quartz crystal in the system which has been used to monitor thickness of the deposited material. The deposition rate and film thickness have been measured with this thickness monitor. As for the growth temperature, substrate surface has been heated by passing electric current through the sample holder. And the temperature of the substrate has been measured by means of thermocouple which was in contact with the sample holder. The deposition rate and the substrate temperature have been varied with the applied voltage value.

In order to produce macroscopically homogeneous films, rotation of sample holder has been advised [21,33]. However, since this rotation is not possible in this system, we have deposited films in all six sections of the sample holder. Then, we have continued to our experiments in the two sections where the deposited films showed macroscopic homogeneity.

2.3 Atomic Force Microscopy

Atomic force microscopy (AFM) is a technique used to map surface properties such as topographical, electrical and magnetic characteristics [41,42]. In our study, we have utilized AFM in order to characterize the surface topography of gold films deposited onto the quartz surfaces. We have used two different AFM instruments namely PSIA XE-100E model from Park Systems and Multi Mode SPM Nanoscope IVA model from Veeco Instruments. In order to process the images, as a software, Nanoscope III Version 5.12r.5 has been used for Veeco' microscope and XEI 1.6 has been used for Park Systems' microscope.

AFM's working principle is mainly based on detection and control of the forces between the scanning probe and the sample. For this purpose, a sharp tip is located at the end of a flexible cantilever and the tip scans the surface. Depending on the instrument, either the tip or the sample is the moving part during the scanning process. Then, the interatomic forces between the sample and the tip atoms cause the mechanical deflection of the cantilever. In order to detect the cantilever displacement, a laser beam is directed to the rear side of the cantilever and the specularly reflected beam is sent to the position sensitive photodetector by the help of a mirror. The output signal coming from photodetector gives the measure of displacement. For topography measurements, it gives the relative height of the scanned surface point. There is a calibration between voltage and

height. Then, this voltage output is processed by a feedback mechanism according to the set point value by which the forces between the tip and the sample are controlled. And the difference is compensated by the output signal of the feedback loop sent to the piezoelectric transducers which controls the relative spatial positions of the tip and the sample. At the end of the scanning process, the computer with a special software convert these measured electrical signals into images [31, 41]. The figure 2.3 shows general operation schematic of AFM.

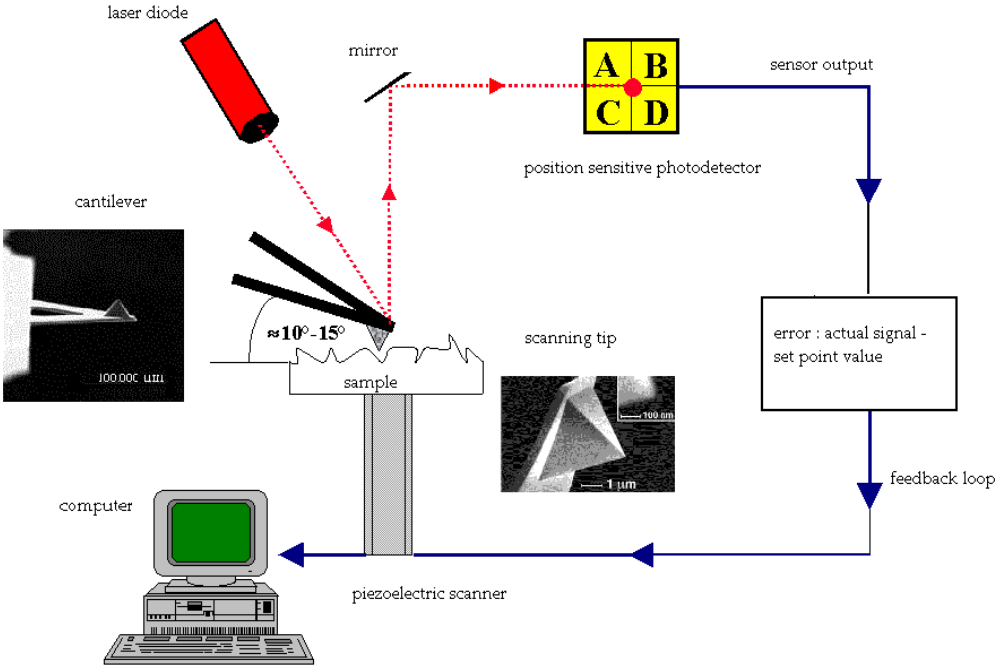

Figure 2.3. Schematic representation of general components of an AFM analysis. Figure is reproduced from ref. 43.

According to the range of tip-to-sample distance, AFM operates in three different modes named as contact, non-contact and tapping modes [31]. The figure 2.4.

shows how van der Waals force changes qualitatively depending on interatomic distance that belogs to different operation modes. In our study, we have operated with tapping mode and especially contact mode.

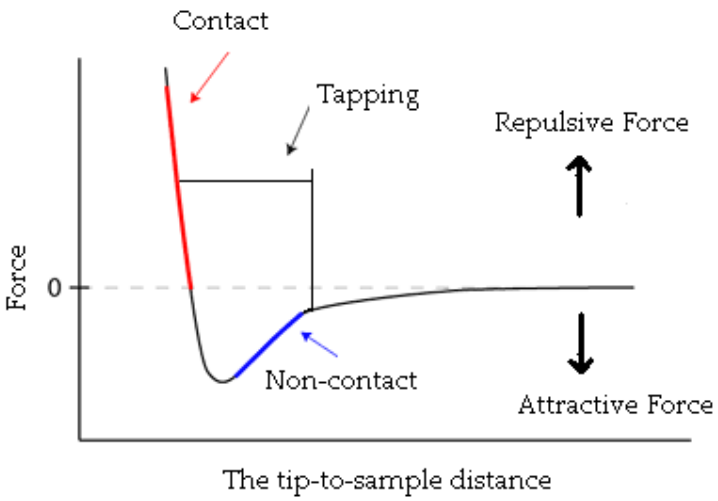

Figure 2.4. Qualitative dependency between interatomic distance and van der Waals force, and the working regions of different operation modes. Figure is reproduced from ref. 31.

2.3.1. Tapping Mode

In tapping mode, the cantilever tip oscillates at its resonance frequency by barely touching to the sample surface. This mode is generally preferred to scan highly corrugated surfaces. Due to the interatomic forces, there occurs a shift in its resonance frequency and this difference gives the height of the scanned sample point. This mode is generally preferred to scan highly corrugated rough surfaces [31,41]. In order to obtain topography images in tapping mode, we have used doped silicon AFM probe with properties shown in the table 2.1.

Table 2.1. AFM probe properties for tapping mode.

Thickness	4 ± 1 μm
Length	125 ± 10 μm
Width	30 ± 7.5 μm
Resonance Frequency	204 - 497 kHz
Force Constant	10 - 130 N/m
Tip Height	10 - 15 μm

2.3.2. Contact Mode

In contact mode, the AFM tip is almost in a physical contact with the sample surface. During scanning, interatomic forces between the tip and the sample atoms cause the cantilever to deflect since it has a spring constant smaller than effective spring constant of the sample atom bonding. There are two operation options in this mode namely constant-height and constant-force. Contact mode is generally preferred to scan flat surfaces [31,41]. In order to obtain topography images in contact mode, we have used doped silicon AFM probe with properties shown in the table 2.2.

Table 2.2. AFM probe properties for contact mode.

Thickness	2.0 ± 1 μm
Length	450 ± 10 μm
Width	50 ± 7.5 μm
Resonance Frequency	6 - 21 kHz
Force Constant	0.02 – 0.77 N/m
Tip Height	10 - 15 μm

As for the AFM images, we have utilized topography images obtained by tapping and contact mode, and deflection images obtained by contact mode. We have scanned square areas on each film with dimensions of 10 μm x 10 μm, 1 μm x 1 μm and 500 nm x 500 nm. And for each scan size, we have scanned at least three different regions on the film separated with a distance of mm range. Before analysis, images have been flattened on the first order. Then, in order to detect gold surfaces having atomically flat regions and small surface corrugation, in AFM analysis, we have focused on grain size and roughness analysis. Firstly, we have scanned 10 μm x 10 μm areas on gold films in order to confirm the microscopic homogeneity of the film and detect the large grains with small surface corrugation. Then, we have scanned 1 μm x 1 μm and 500 nm x 500 nm areas on gold films by focusing on only these large grains having atomically flat regions. For this reason, although the same film was scanned, as the scan size changed, the roughness value changed for some films.

For roughness analysis, we have utilized root mean square (rms) roughness. It is the standard deviations of the height values according to the mean data plane and calculated by the below formula:

$$\sqrt{\frac{\sum Z_i^2}{n}} = R_q \qquad (2.1.)$$

where n is the number of data points on the scanned surface and Z_i is the height value relative to mean data plane that belongs to each data point [44]. The reported roughness values are the averages of three roughness values belonging to three different regions on the film for each scan size. And the accompanying z scale values represent the controlled height difference between the highest and lowest points on the scanned surface which corresponds to the full extent of the color scale [44]. As for the grain size, it has been evaluated qualitatively as being the area of the separated gold groups which can be differentiated by eye from AFM images.

CHAPTER 3

RESULTS AND DISCUSSION

In this chapter, the effect of the studied deposition parameters on the morphology of the gold films deposited onto quartz surfaces will be evaluated separately for electron beam and thermal deposition methods taking into account their AFM images. As the starting deposition parameters, the ones in the study of Danışman [30] have been utilized.

3.1. Gold Films Deposited by Electron Beam Deposition Method

3.1.1. Effect of Substrate Temperature

Effect of substrate temperature on the morphology of 100 nm thick gold films deposited onto quartz surfaces with a deposition rate of 0.3±0.03 Å/s has been investigated. One set of films has been deposited at a substrate temperature of 250±5 ^{0}C and the other set has been deposited at a substrate temperature of 400±5 ^{0}C. The corresponding contact mode AFM images are shown in figure 3.1.

We have observed that at high growth temperature of 400±5 ^{0}C, grain size and roughness increased. The reason for these can be explained as follows: At low deposition rate, the number of nucleation sites is small. However, at high temperature with the increased diffusion of atoms, this number might be even

smaller. In such a case, instead of layer formation, film growth occurs as island growth around smaller number of nucleation sites. And this brings an increase in grain size causing a sharp increase in roughness. The result is in parallel with the literature studies [23,24,26].

Substrate Temperature of 250±5 ^{0}C **Substrate Temperature of 400±5 ^{0}C**

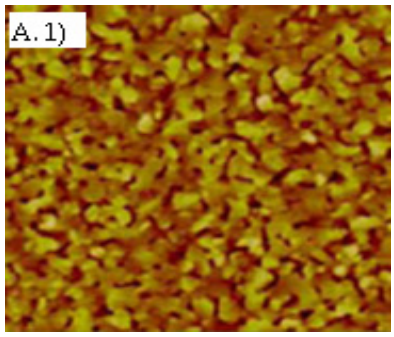

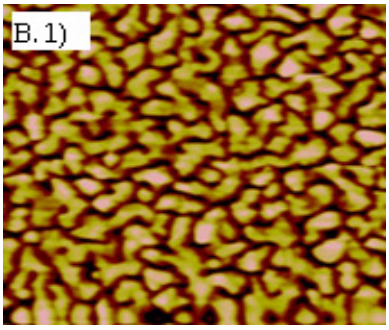

R_q : 13.2±1.3 nm ; Z-scale : 141 nm R_q : 42.2±1.5 nm ; Z-scale : 141 nm

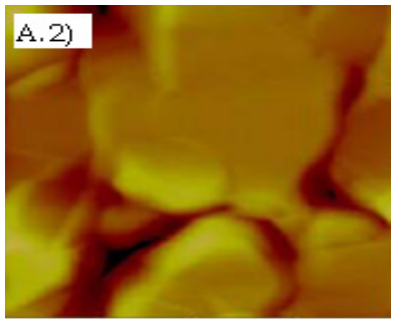

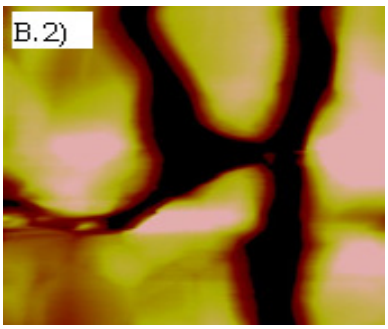

R_q : 11.8±0.9 nm ; Z-scale : 108 nm R_q : 49.1±2.3 nm ; Z-scale : 108 nm

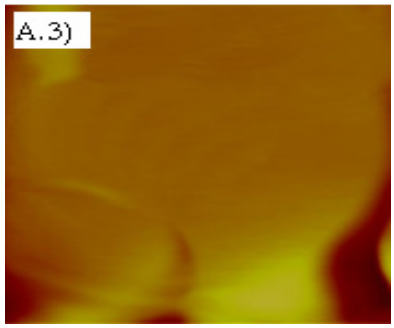

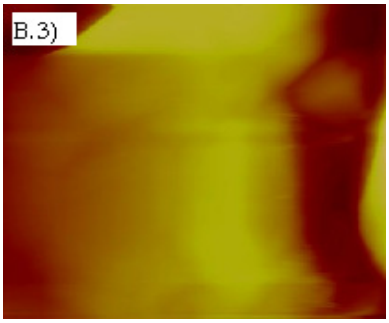

R_q : 3.8±0.4 nm ; Z-scale : 70 nm R_q : 38.0±1.6 nm ; Z-scale : 250 nm

Figure 3.1. AFM images for gold films deposited at the substrate temperature of 250±5 ^{0}C (A) and 400±5 ^{0}C (B). Scan size of the images are 10 μm x 10 μm (1), 1 μm x 1 μm (2) and 500 nm x 500 nm (3).

3.1.2. Effect of Adhesive Layer

Effect of adhesive layer on the morphology of 100 nm thick gold films deposited onto quartz surfaces at a substrate temperature of 250±5 ^{0}C and with a deposition rate of 0.3±0.03 Å/s has been investigated. One set of films has been deposited directly onto the quartz surface and the other set has been deposited onto about 6 nm thick chromium layer deposited quartz surface. This 6 nm thick chromium layer has been deposited by electron beam deposition method with a deposition rate of 0.4±0.03 Å/s without heating the quartz surface. In all experiments where the adhesive layer has been used, the same procedure has been applied regarding chromium deposition. The corresponding contact mode AFM images are shown in figure 3.2.

We have observed that in the presence of adhesive layer, grain size decreased and roughness increased. The reason for these might be related to decreased diffusion of gold atoms since they are strongly adsorbed onto chromium layer. Then, film growth occurs as island growth by resulting in a film with smaller grain size and higher roughness value.

Without Adhesive Layer **With Adhesive Layer**

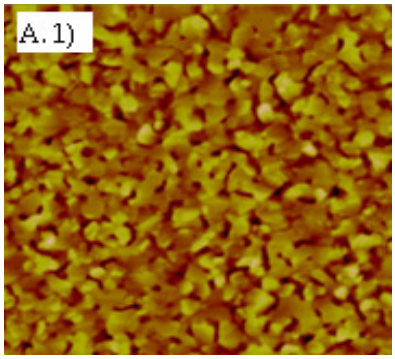

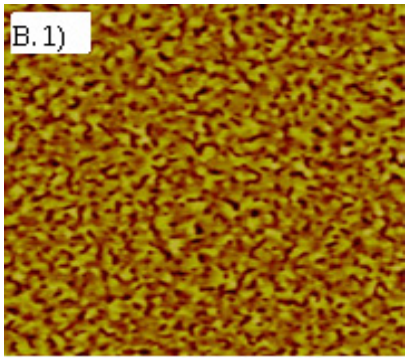

R_q : 13.2±1.3 nm ; Z-scale : 100 nm

R_q : 25.6±1.2 nm ; Z-scale : 100 nm

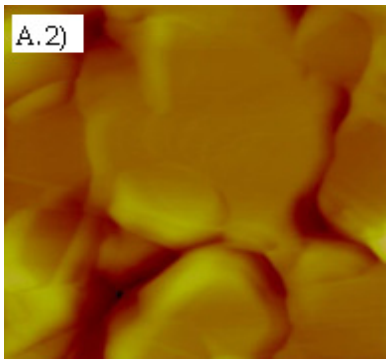

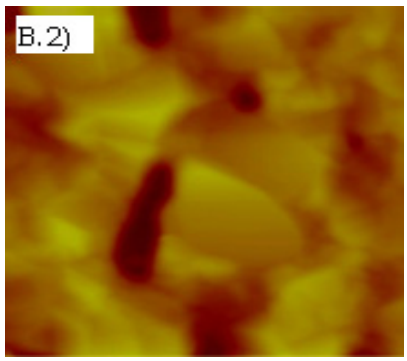

R_q : 11.8±0.9 nm ; Z-scale : 140 nm

R_q : 21.3±0.8 nm ; Z-scale : 140 nm

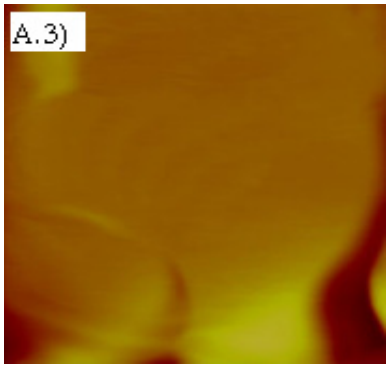

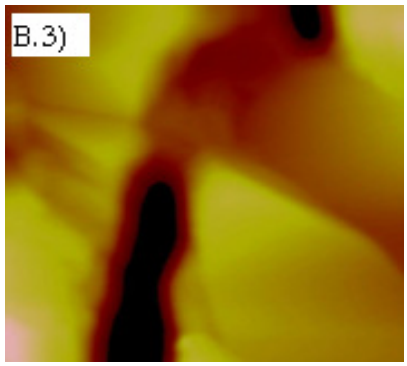

R_q : 3.8±0.4 nm ; Z-scale : 70 nm

R_q : 15.5±1.1 nm ; Z-scale : 70 nm

Figure 3.2. AFM images for gold films without adhesive layer (A) and with adhesive layer (B). Scan size of the images are 10 μm x 10 μm (1), 1 μm x 1 μm (2) and 500 nm x 500 nm (3).

3.1.3. Effect of Substrate Temperature in The Presence of Adhesive Layer

Effect of substrate temperature on the morphology of 100 nm thick gold films deposited onto chromium deposited quartz surfaces with a deposition rate of 0.3±0.03 Å/s has been investigated. One set of films has been deposited at a substrate temperature of 70±8 ^{0}C and the other set has been deposited at a substrate temperature of 250±5 ^{0}C. The corresponding contact mode AFM images are shown in figure 3.3.

We have observed that at low growth temperature of 70±8 ^{0}C, grain size and roughness decreased dramatically. The decreased grain size might be explained as follows: The number of nucleation sites might remain nearly constant since diffusion of gold atoms decrease at this low temperature compared to the diffusion at 250±5 ^{0}C and film growth occurs around the present nucleation sites causing grain formation with smaller size again due to this lower diffusion rate. Consequently, gold atoms wet the chromium layer better in the presence of higher nucleation sites by limiting the growth in vertical direction (which is the normal to the film surface). And this brings a decrease in roughness.

Substrate Temperature of 70±8 ^{0}C **Substrate Temperature of 250±5 ^{0}C**

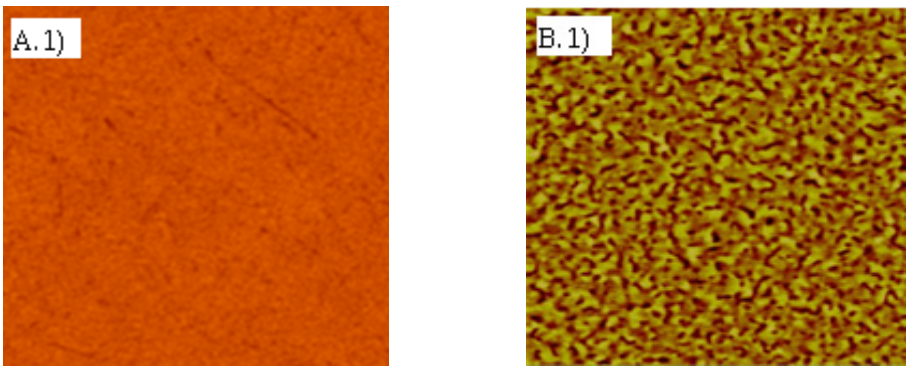

R_q : 1.4±0.1 nm ; Z-scale : 100 nm R_q : 25.6±1.2 nm ; Z-scale : 100 nm

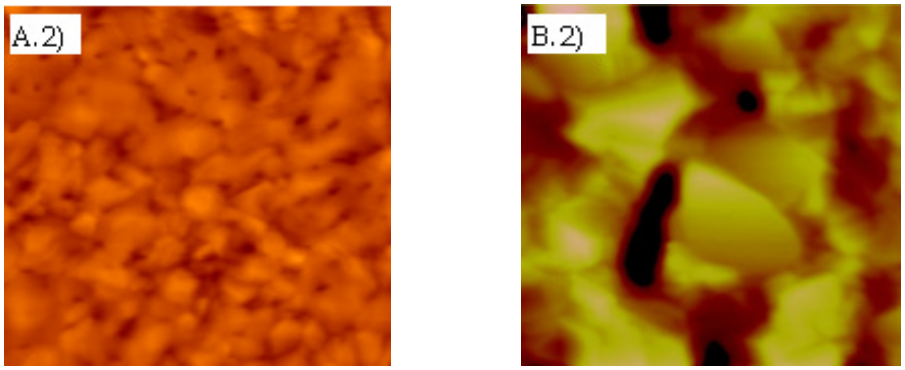

R_q : 2.6±0.2 nm ; Z-scale : 65 nm R_q : 21.3±0.8 nm ; Z-scale : 65 nm

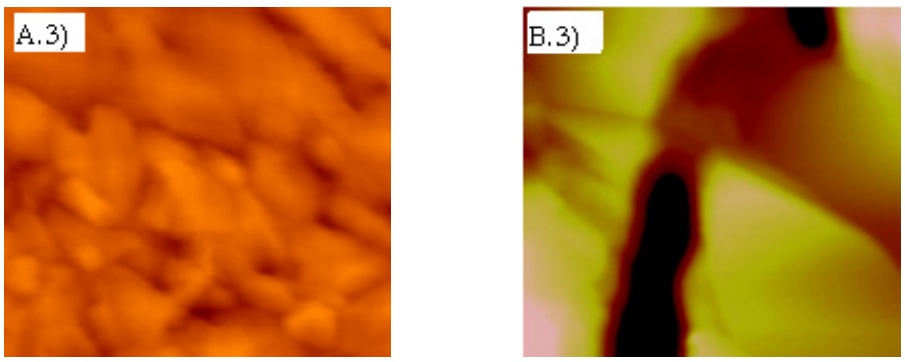

R_q : 2.0±0.2 nm ; Z-scale : 49 nm R_q : 15.5±1.1 nm ; Z-scale : 49 nm

Figure 3.3. AFM images for gold films deposited at the substrate temperature of 70±8 ^{0}C (A) and 250±5 ^{0}C (B) in the presence of adhesive layer. Scan size of the images are 10 μm x 10 μm (1), 1 μm x 1 μm (2) and 500 nm x 500 nm (3).

3.1.4. Effect of Deposition Rate in The Presence of Adhesive Layer

Effect of deposition rate on the morphology of 100 nm thick gold films deposited onto chromium deposited quartz surfaces at a substrate temperature of 70±8 ^{0}C has been investigated. One set of films has been deposited with a deposition rate of 0.3±0.03 Å/s and the other set has been deposited with a deposition rate of 5.0±0.03 Å/s. The corresponding contact mode AFM images are shown in figure 3.4.

We have observed that at high deposition rate of 5.0±0.03 Å/s, roughness value and grain size decreased. The reason for the decrease in grain size might be related to that gold atoms prefer to form smaller grains around higher number of nucleation sites instead of diffusing on the adhesive layer compared to the presence of smaller number of nucleation sites resulted at a deposition rate of 0.3±0.03 Å/s. The reason for this might be that they do not have to reach the separated small number of nucleation sites as in the case of low deposition rate due to the closely located high number of nucleation sites. As for the decrease in roughness, the reason can be explained as follows: In the presence of high nucleation sites, the distance between the grains is smaller. When this is accompanied with the good wetting property of adsorbate, the diffusion along vertical direction (which is the normal to the film surface) is limited by the availability of easy diffusion on the horizontal plane (which is the film surface). And this might cause a slight decrease in roughness. The result is in parallel with the literature studies [27,37,38].

Deposition Rate of 0.3±0.03 Å/s | **Deposition Rate of 5.0±0.03 Å/s**

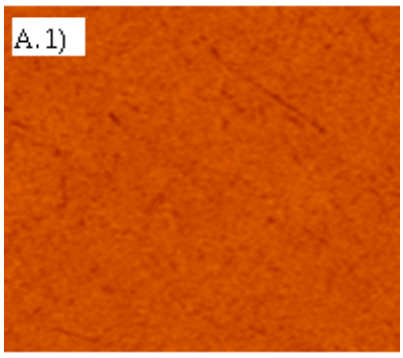

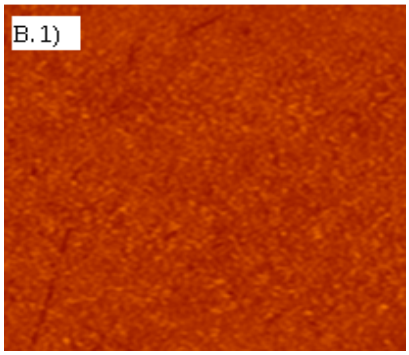

R_q : 1.4±0.1 nm ; Z-scale : 100 nm

R_q : 2.1±0.1 nm ; Z-scale : 100 nm

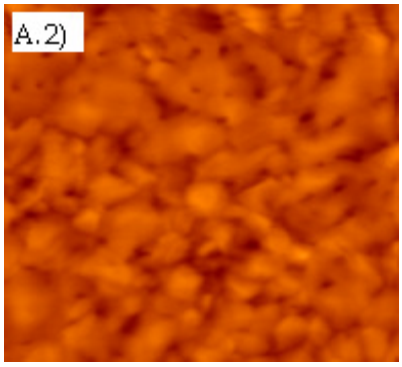

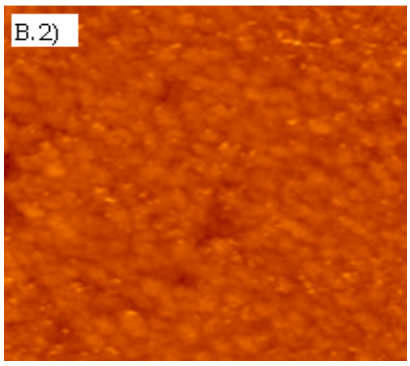

R_q : 2.6±0.2 nm ; Z-scale : 65 nm

R_q : 1.6±0.2 nm ; Z-scale : 65 nm

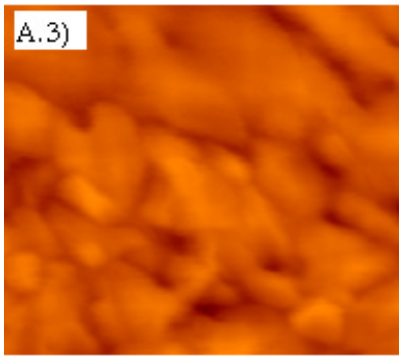

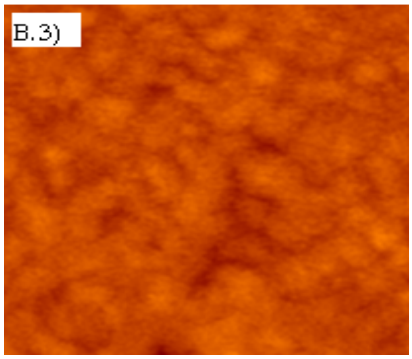

R_q : 2.0±0.2 nm ; Z-scale : 49 nm

R_q : 1.3±0.1 nm ; Z-scale : 49 nm

Figure 3.4. AFM images for gold films deposited with a deposition rate of 0.3±0.03 Å/s (A) and 5.0±0.03 Å/s (B) in the presence of adhesive layer. Scan size of the images are 10 μm x 10 μm (1), 1 μm x 1 μm (2) and 500 nm x 500 nm (3).

3.1.5. Effect of Annealing in The Presence of Adhesive Layer

Effect of annealing on the morphology of 100 nm thick gold films deposited onto chromium deposited quartz surfaces at a substrate temperature of 70±8 ^{0}C has been investigated. All films have been deposited with a deposition rate of 5.0±0.03 Å/s. Then, among three sets of film, one set of film has been annealed with oxygen-acetylene flame at 850±20 ^{0}C for 2 minutes in a ceramic crucible. The temperature has been measured by means of thermocouple which was in contact with the base of the crucible. And the other set has been annealed in oven under nitrogen atmosphere at 850±1 ^{0}C for 15 minutes. The corresponding tapping mode AFM images are shown in figure 3.5.

Actually, firstly, we have tried to simulate the starting gold film stated in the study of Lauer et al. [25] and by applying flame annealing, we have aimed to increase the grain size and decrease the roughness value. However, in flame annealing process, quartz crystal was broken after about 2 minutes. As for the reason of this, we have concluded that the thin quartz crystal could not tolerate the stress caused by suddenly increased temperature and nonhomogeneous temperature distribution in flame condition accompanied with high temperature. The AFM analysis regarding the effect of flame annealing has been performed on the broken piece of quartz. Then, we have tried to achieve annealing in oven since we have a limitation about quartz thickness regarding QCM application. The used AT cut quartz crystals have a special resonance frequency for QCM application and consequently have a fixed thickness [30].

We have observed that both flame annealing and annealing in oven at 850±1 ^{0}C caused an increase in both roughness value and grain size. As for the annealing in oven, the reason of increase in grain size and roughness might be related to the long time provided in oven condition for diffusion of chromium atoms into

the gold film in addition to diffusion of gold atoms [34]. As for the flame annealing, although we have analyzed the resulted image, we have concluded that it is not applicable for a thin quartz crystal.

Nonannealed Film

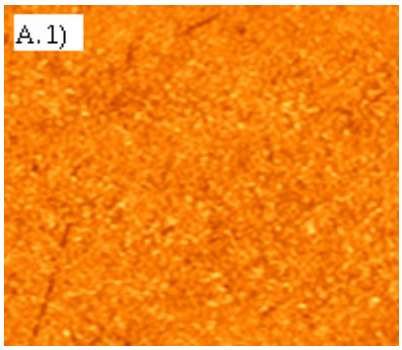

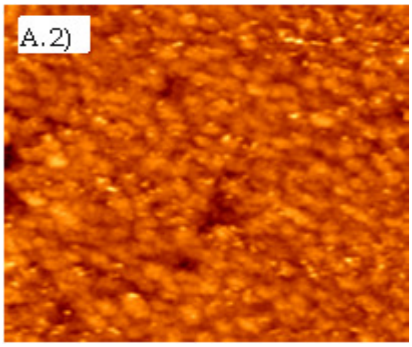

R_q : 2.1±0.1 nm ; Z-scale : 50 nm

R_q : 1.6±0.2 nm ; Z-scale : 25 nm

Annealed Film with Flame

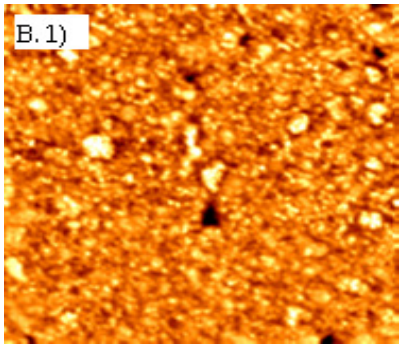

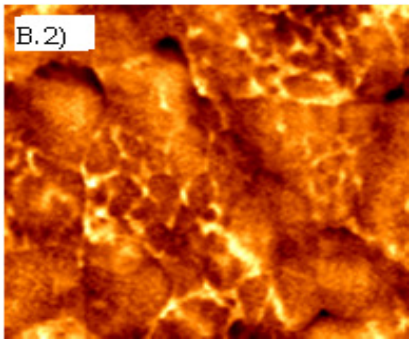

R_q : 6.2±0.5 nm ; Z-scale : 50 nm

R_q : 2.9±0.3 nm ; Z-scale : 25 nm

Annealed Film in Oven

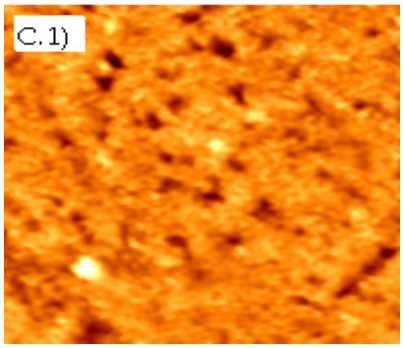

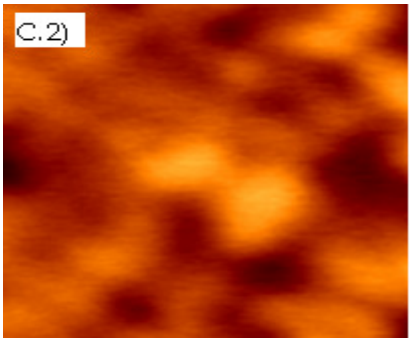

R_q : 3.7±0.3 nm ; Z-scale : 50 nm

R_q : 2.1±0.2 nm ; Z-scale : 25 nm

Figure 3.5. AFM images for gold films nonannealed (A), flame annealed (B) and annealed in oven (C) in the presence of adhesive layer. Scan size of the images are 10 μm x 10 μm (1) and 1 μm x 1 μm (2).

3.1.6. Effect of Prebaking of Quartz Surface Before Deposition

Effect of quartz prebaking on the morphology of 100 nm thick gold films deposited onto quartz surfaces at a substrate temperature of 250±5 ^{0}C and with a deposition rate of 0.3±0.03 Å/s has been investigated. One set of films has been deposited directly onto the quartz surface and the other set has been deposited onto the quartz surface prebaked before deposition between 300-350 ^{0}C for 4 hours. The corresponding contact mode AFM images are shown in figure 3.6.

We have observed that prebaking of quartz surface before deposition caused a decrease in roughness of gold film thanks to the removal of adsorbed contaminants from the quartz surface as we have expected. However, surprisingly , we have observed a decrease in grain size. From the AFM images, we have concluded that the only reason for this might be the increased deposition rate although we have not changed the rate. In accordance with this observation, we have done successive experiments. However, the result did not changed and we have faced with reproducibility problem. Compared to the previous ones, the only difference of the last depositions was the sharp increase in deposition rate during deposition process. This might be related to a problem regarding electrical connections of the evaporator. And, we have concluded that although we compensated for the increase as fast as possible, this high rate might create high number of nucleation sites causing smaller grain size. After this technical problem which we were not able to solve, we have focused on the thermal deposition method. And with thermal method, we have not investigated the effect of use of adhesive layer and annealing which did not give desired results in electron beam deposition method.

Nonprebaked Quartz **Prebaked Quartz**

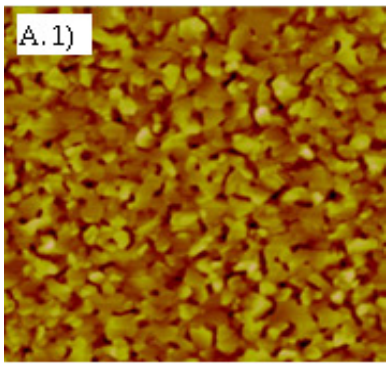

R_q : 13.2±1.3 nm ; Z-scale : 100 nm

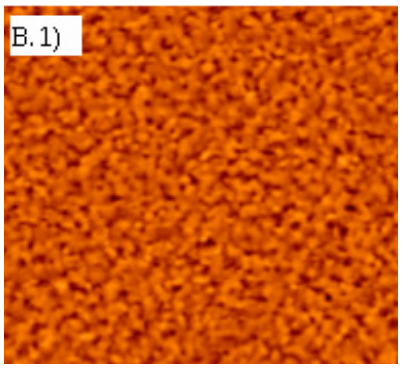

R_q : 5.5±0.4 nm ; Z-scale : 100 nm

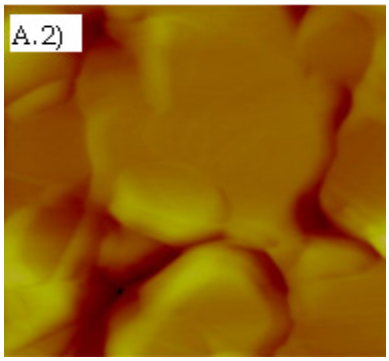

R_q : 11.8±0.9 nm ; Z-scale : 140 nm

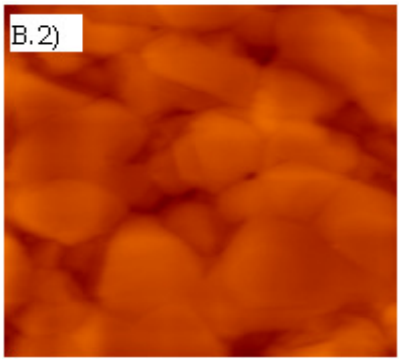

R_q : 5.1±0.3 nm ; Z-scale : 140 nm

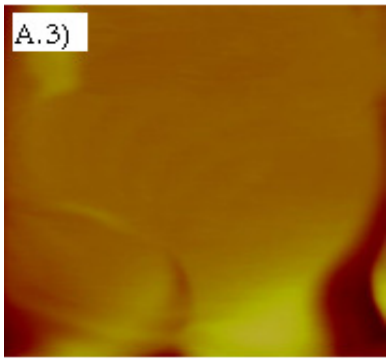

R_q : 3.8±0.4 nm ; Z-scale : 70 nm

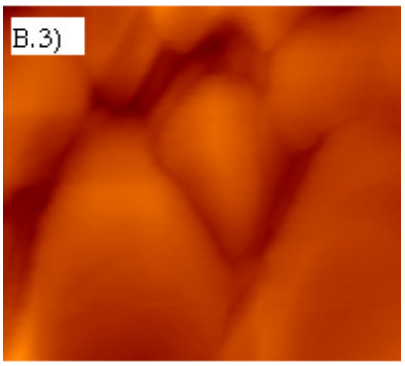

R_q : 3.1±0.3 nm ; Z-scale : 70 nm

Figure 3.6. AFM images for gold films deposited directly onto the quartz surface (A) and onto the prebaked quartz surface (B). Scan size of the images are 10 μm x 10 μm (1), 1 μm x 1 μm (2) and 500 nm x 500 nm (3).

3.2. Gold Films Deposited by Thermal Deposition Method

3.2.1. Effect of Prebaking of Quartz Surface Before Deposition

Effect of quartz prebaking on the morphology of 100 nm thick gold films deposited onto quartz surfaces at a substrate temperature of 250±5 ^{0}C and with a deposition rate of 0.3±0.03 Å/s has been investigated. One set of films has been deposited directly onto the quartz surface and the other set has been deposited onto the quartz surface prebaked before deposition between 300-350 ^{0}C for 4 hours. The corresponding contact mode AFM images are shown in figure 3.7.

We have observed that prebaking of quartz surface before deposition caused a decrease in roughness thanks to removal of contaminants from the quartz surface as it was expected. The result is in parallel with the literature studies [24,27].

By taking into account the lowered roughness value, the effect of substrate temperature, deposition rate and film thickness have been investigated on the prebaked quartz surface.

Nonprebaked Quartz **Prebaked Quartz**

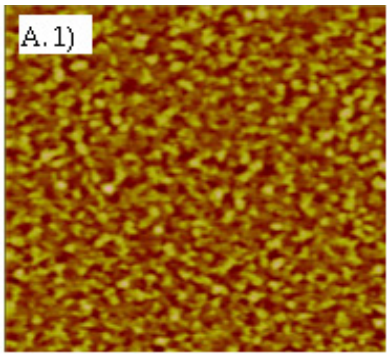

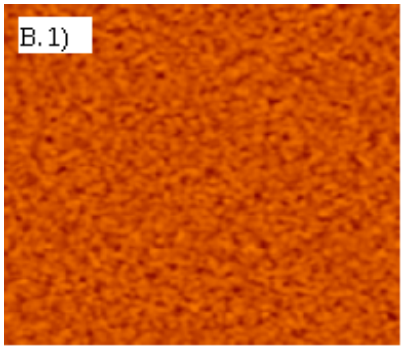

R_q : 11.4±1.1 nm ; Z-scale : 100 nm R_q : 3.2±0.3 nm ; Z-scale : 100 nm

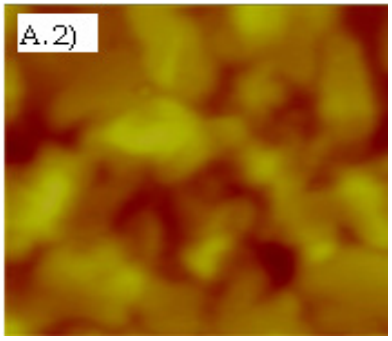

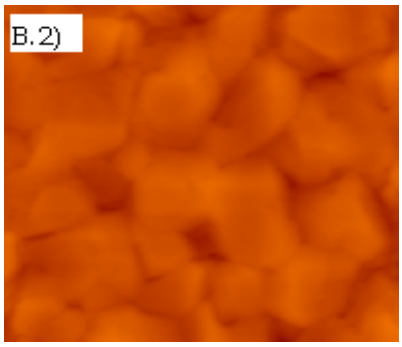

R_q : 10.9±1.4 nm ; Z-scale : 140 nm R_q : 3.6±0.4 nm ; Z-scale : 140 nm

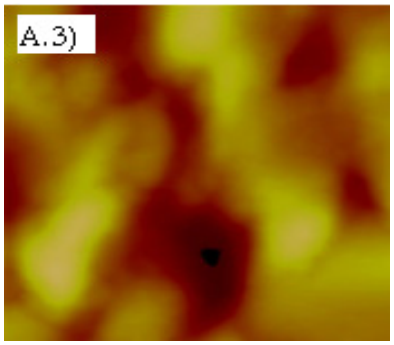

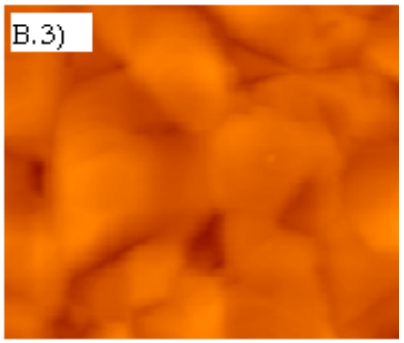

R_q : 8.4±1.5 nm ; Z-scale : 70 nm R_q : 2.5±0.4 nm ; Z-scale : 70 nm

Figure 3.7. AFM images for gold films deposited directly onto the quartz surface (A) and onto the prebaked quartz surface (B) by thermal evaporation method. Scan size of the images are 10 μm x 10 μm (1), 1 μm x 1 μm (2) and 500 nm x 500 nm (3).

3.2.2. Effect of Substrate Temperature

Effect of substrate temperature (T_S) on the morphology of 100 nm thick gold films deposited onto prebaked quartz surfaces with a deposition rate of 0.3±0.03 Å/s has been investigated. First set of films has been deposited at a substrate temperature of 70±8 ^{0}C, second set of films has been deposited at a substrate temperature of 250±5 ^{0}C and the final set has been deposited at a substrate temperature of 400±5 ^{0}C. The corresponding contact mode AFM images are shown in figure 3.8.

We have observed that as the substrate temperature increased, grain size and roughness increased. The reason for the increase in grain size might be that diffusion of gold atoms increases as the substrate temperature increases. As for the increase in roughness, the reason might be the decrease in the number of nucleation sites depending on increased diffusion of gold atoms on the prebaked quartz surface with the increased temperature and the resulted island growth. The result is in parallel with the literature studies [27,36,38].

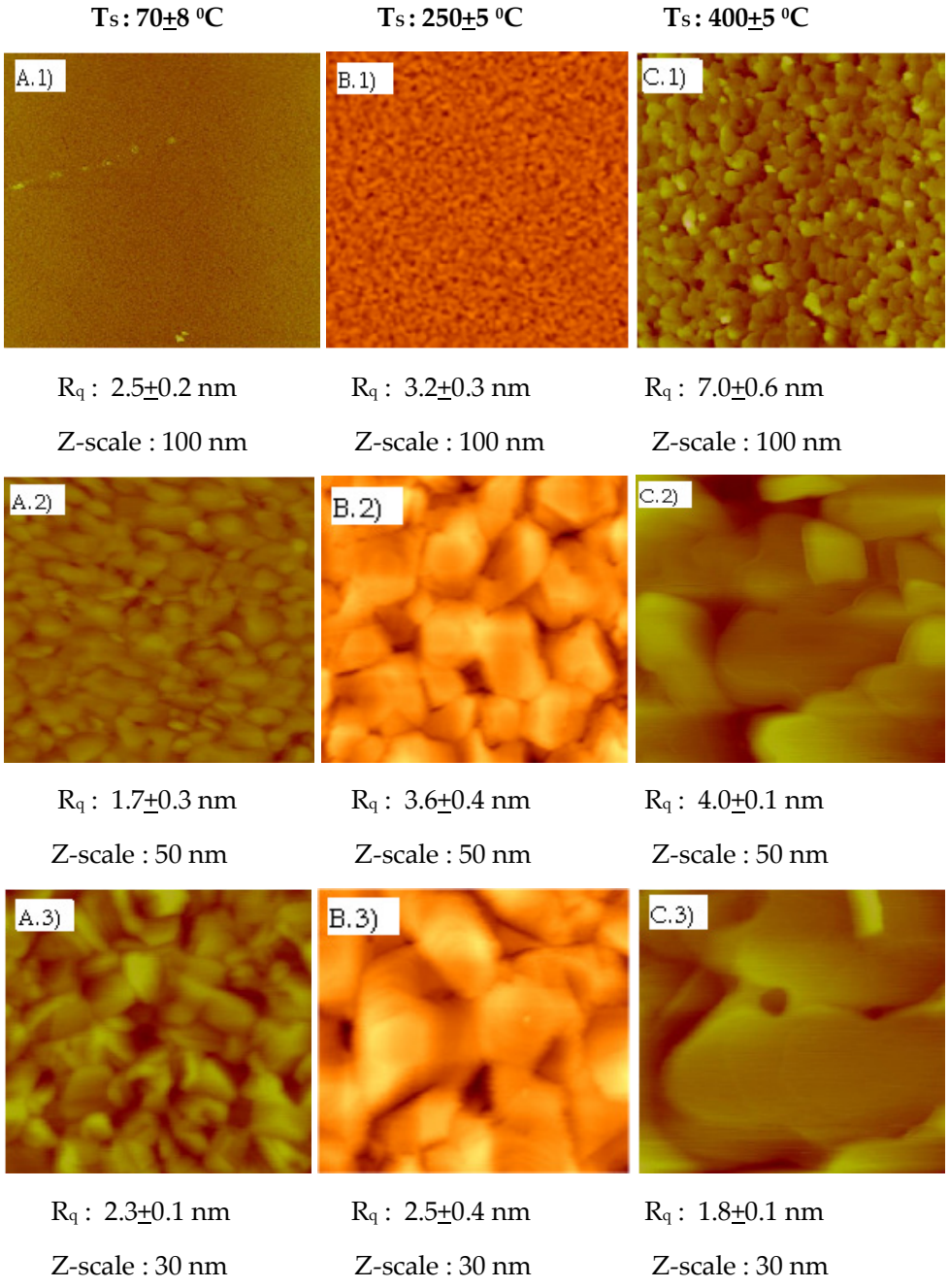

Figure 3.8. AFM images for gold films deposited onto the prebaked quartz surface at the substrate temperature of 70±8 °C (A), 250±5 °C (B) and 400±5 °C (C). Scan size of the images are 10 μm x 10 μm (1), 1 μm x 1 μm (2) and 500 nm x 500 nm (3).

3.2.3. Effect of Deposition Rate

Effect of deposition rate on the morphology of 100 nm thick gold films deposited onto prebaked quartz surfaces at a substrate temperature of 250±5 ^{0}C has been investigated. One set of films has been deposited with a deposition rate of 0.3±0.03 Å/s and the other set has been deposited with a deposition rate of 5.0±0.03 Å/s. This high rate has been chosen in order to be able to observe the effect of deposition rate more clearly. The corresponding contact mode AFM images are shown in figure 3.9.

We have observed that high deposition rate of 5.0±0.03 Å/s caused a slight decrease in roughness value and grain size. The reasons for these are as stated in the case of electron beam deposition. The reason for the decrease in grain size might be related to that gold atoms prefer to form smaller grains around high number of nucleation sites instead of diffusing since they do not have to reach the separated small number of nucleation sites as in the case of low deposition rate due to the closely located high number of nucleation sites. As for the decrease in roughness, the reason can be explained as follows: In the presence of high nucleation sites, the distance between the grains is smaller. When this is accompanied with the good wetting property of adsorbate, the diffusion along vertical direction (which is the normal to the film surface) is limited by the availability of easy diffusion on the horizontal plane (which is the film surface). And this might cause a slight decrease in roughness. The result is in parallel with the literature studies [27,37,38].

Deposition Rate of 0.3±0.03 Å/s

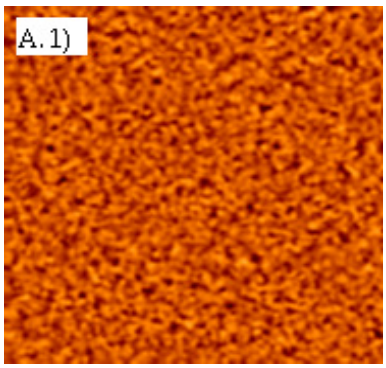

R_q : 3.2±0.3 nm ; Z-scale : 50 nm

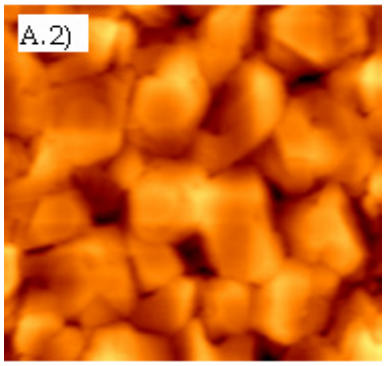

R_q : 3.6±0.4 nm ; Z-scale : 40 nm

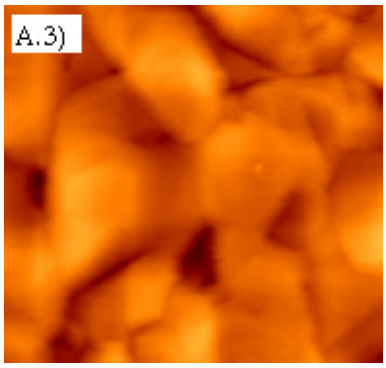

R_q : 2.5±0.4 nm ; Z-scale : 40 nm

Deposition Rate of 5.0±0.03 Å/s

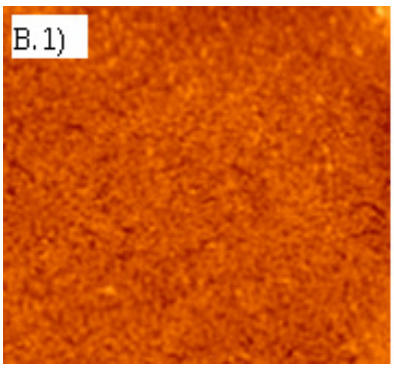

R_q : 1.7±0.2 nm ; Z-scale : 50 nm

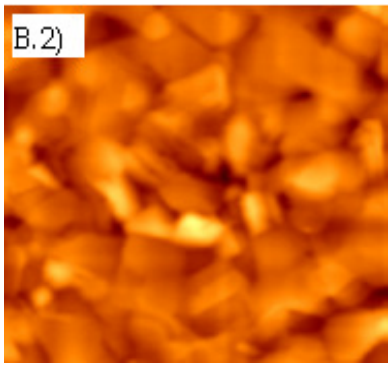

R_q : 2.5±0.3 nm ; Z-scale : 40 nm

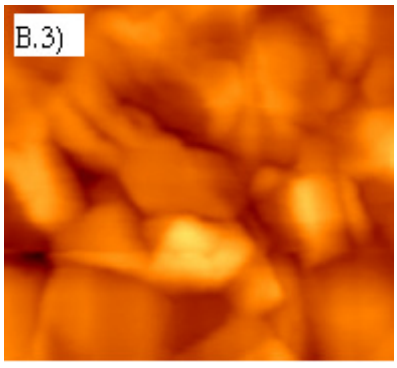

R_q : 2.5±0.2 nm ; Z-scale : 40 nm

Figure 3.9. AFM images for gold films deposited onto the prebaked quartz surface with a deposition rate of 0.3±0.03 Å/s (A) and 5.0±0.03 Å/s (B). Scan size of the images are 10 μm x 10 μm (1), 1 μm x 1 μm (2) and 500 nm x 500 nm (3).

3.2.4. Effect of Film Thickness

Effect of film thickness on the morphology of gold films deposited onto prebaked quartz surfaces at a substrate temperature of 400±5 ^{0}C and with a deposition rate of 0.3±0.03 Å/s has been investigated. One set of films has been deposited with a thickness of 100 nm and the other set has been deposited with a thickness of 50 nm. The corresponding contact mode AFM images are shown in figure 3.10.

We have found that low film thickness of 50 nm caused a decrease in grain size and a slight difference in roughness value. As for the effect of film thickness, it is known that it changes depending on the growth mode. For this reason, we have concluded that the decrease in grain size might be the sign of layer plus island growth observed at these deposition parameters. By looking at growth modes [31], we can say that film thickness of 50 nm might represents for the island formation; i.e. the period before layer formation at these deposition parameters. And this also explains the slight increase in roughness observed in small scale.

Film Thickness of 100 nm **Film Thickness of 50 nm**

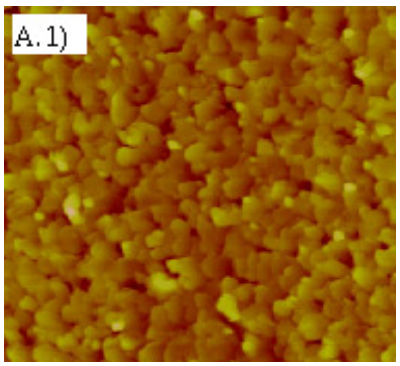

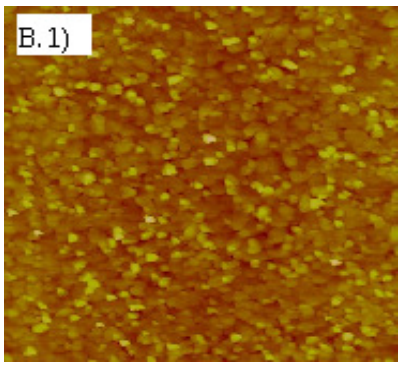

R_q : 7.0±0.6 nm ; Z-scale : 100 nm R_q : 6.0±0.4 nm ; Z-scale : 100 nm

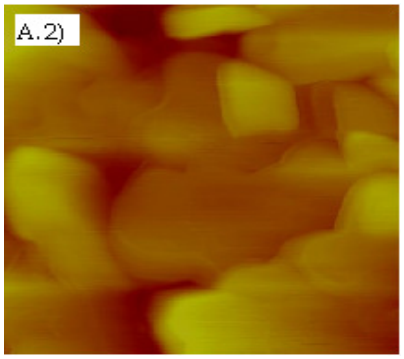

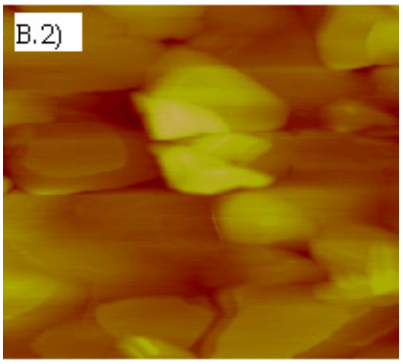

R_q : 4.0±0.1 nm ; Z-scale : 50 nm R_q : 4.1±0.4 nm ; Z-scale : 50 nm

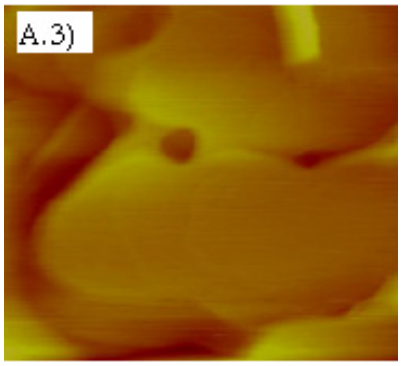

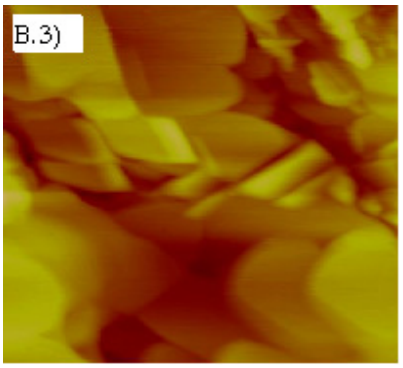

R_q : 1.8±0.1 nm ; Z-scale : 30 nm R_q : 3.1±0.5 nm ; Z-scale : 30 nm

Figure 3.10. AFM images for gold films deposited onto the prebaked quartz surface with a film thickness of 100 nm (A) and 50 nm (B). Scan size of the images are 10 μm x 10 μm (1), 1 μm x 1 μm (2) and 500 nm x 500 nm (3).

3.3. Best Gold Films Produced by Electron Beam and Thermal Deposition Methods

Among the deposited gold films, AFM topography images and the related roughness and z-scale values of the best ones produced by electron beam deposition and thermal deposition methods are shown in the figure 3.11.

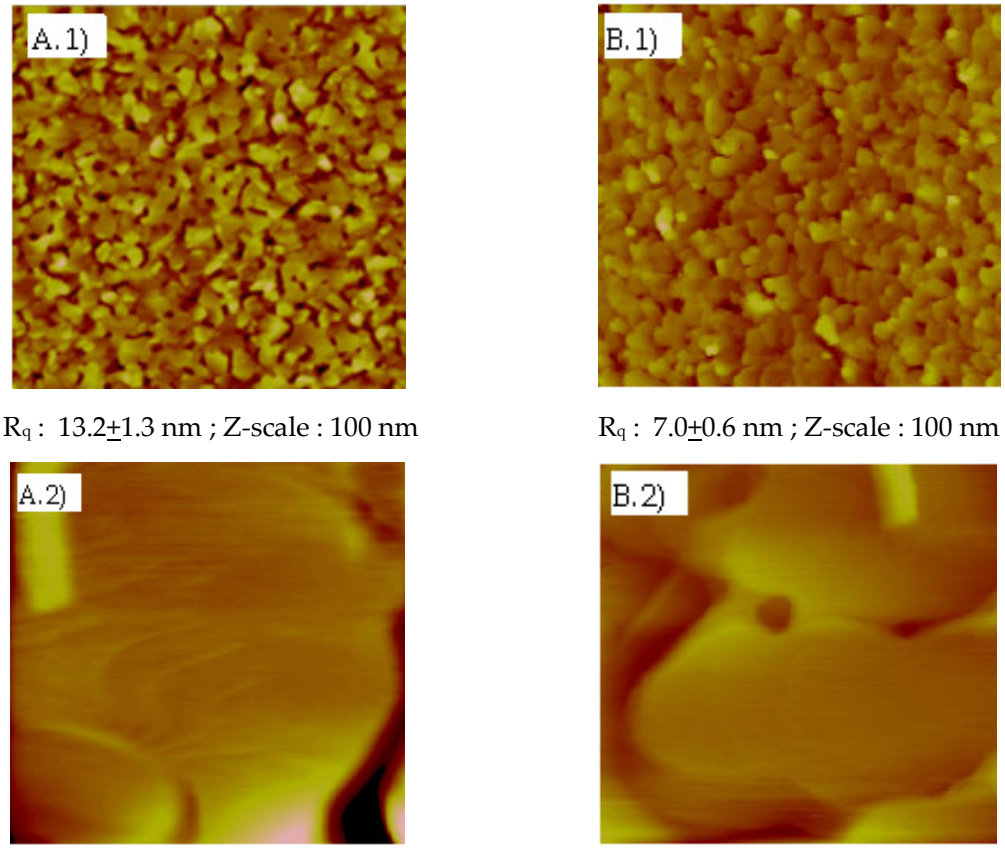

R_q : 13.2±1.3 nm ; Z-scale : 100 nm

R_q : 7.0±0.6 nm ; Z-scale : 100 nm

R_q : 3.8±0.4 nm ; Z-scale : 30 nm

R_q : 1.8±0.1 nm ; Z-scale : 30 nm

Figure 3.11. AFM images for best gold films obtained by electron beam deposition (A) and thermal deposition (B) methods. Scan size of the images are 10 μm x 10 μm (1) and 500 nm x 500 nm (2).

In the case of electron beam deposition, 100 nm thick gold films deposited onto quartz surfaces at a substrate temperature of 250±5 ^{0}C and with a deposition rate of 0.3±0.03 Å/s resulted in the best film morphology by having the largest atomically flat regions with the smallest roughness values. And in the case of thermal deposition, 100 nm thick gold films deposited onto the prebaked quartz surfaces at a substrate temperature of 400±5 ^{0}C and with a deposition rate of 0.3±0.03 Å/s showed the best morphology. As for the detection of atomically flat areas, we have utilized formation of steps on the gold film surface. And we have detected the step like formations from topography images and more clearly from deflection images. Then, we have measured the step height; i.e. the height of one atomic layer in these regions and observed that they varied between 0.200 nm and 0.300 nm although the theoretical value of step height for an atomically flat gold surface is 0.236 nm. However, according to the similar fluctuations stated in the literature [21, 27], we have concluded that these surface features represent step formations and fluctuations might be caused mostly due to the noise during AFM measurements. And, we have reported the minimum values of atomically flat areas with a surface corrugation smaller than 0.200 nm. By electron beam deposition, we have obtained a minimum 90 nm^2 atomically flat gold surface and by thermal deposition, we have obtained a minimum 170 nm^2 atomically flat gold surface. However, by looking at the large terraces in deflection images, we have concluded that these areas might be as large as thousands of nm^2.

The deflection images and topography images with corresponding line profiles belonging to these films are shown in figures 3.12 and 3.13.

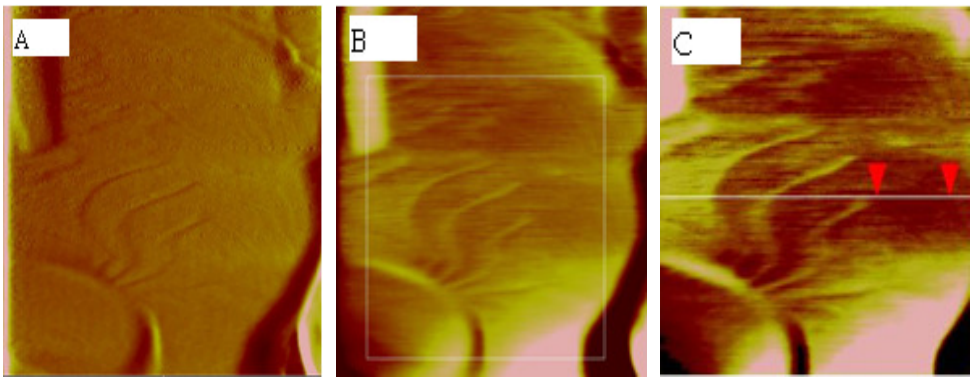

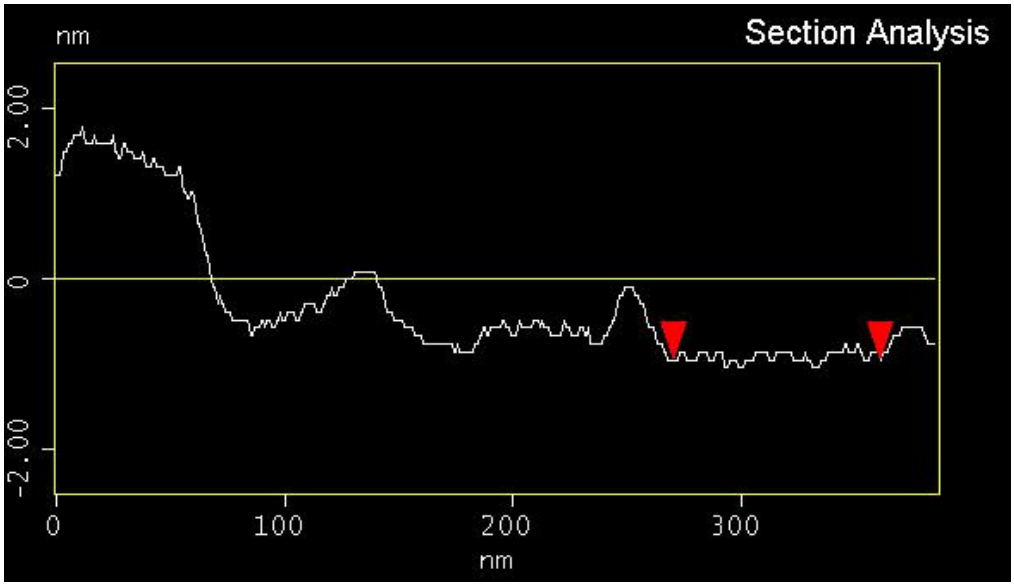

Figure 3.12. AFM deflection image (A), topography image (B) and zoomed topography image (C) with line profile for the gold film deposited by electron beam deposition. All images have a scan size of 500 nm x 500 nm.

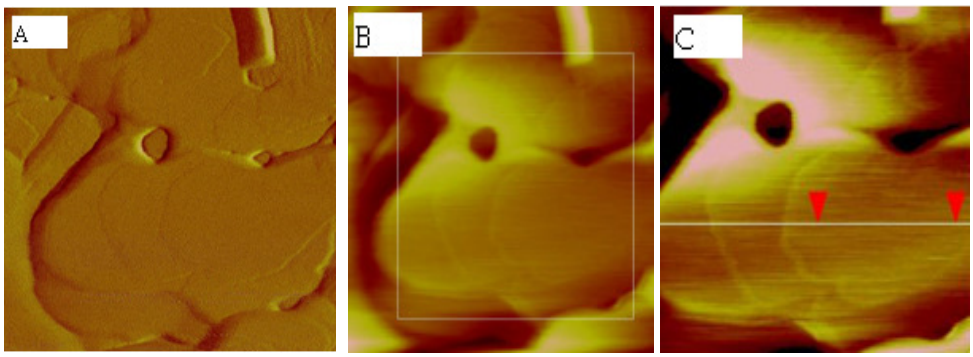

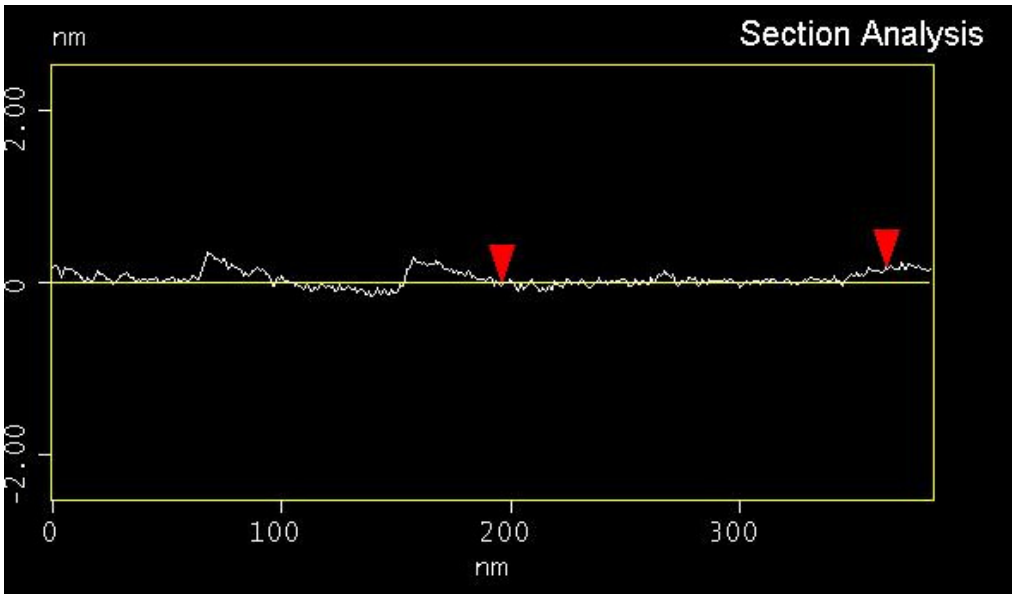

Figure 3.13. AFM deflection image (A), topography image (B) and zoomed topography image (C) with line profile for the gold film deposited by thermal deposition. All images have a scan size of 500 nm x 500 nm.

CHAPTER 4

CONCLUSIONS

In conclusion, in this study, we have deposited gold films onto the quartz surfaces by electron beam and thermal deposition methods. We have studied the effect of substrate temperature, use of adhesive layer, deposition rate, annealing and substrate prebaking on the gold film morphology in our evaporator system.

We have observed that as the substrate temperature increased, grain size and roughness values increased too due to the increased diffusion of gold atoms. We have found that use of adhesive layer provided strong adsorption of gold atoms by resulting in smaller roughness value. We have observed that as the deposition rate increased, grain size decreased. As for the annealing procedure, we could not observe the expected result for flame annealing since it is not applicable for a thin quartz crystal. In the case of annealing in oven, although it is applicable for the used quartz crystal, again we could not observe the healing effect of annealing. Regarding film thickness, we confirmed its growth mode dependency. Finally, we have observed the healing effect of prebaking of quartz surface before deposition on the roughness of gold film. Except annealing procedure, all these results are in parallel with the trends stated in the literature.

Regarding gold film morphology suitable to study simultaneously with quartz crystal microbalance and helium atom diffraction, the deposited films should have mechanical stability, macroscopic homogeneity, large atomically flat surfaces and small roughness value. In accordance with these properties, we have

obtained about a minimum 170 nm^2 atomically flat surface by thermal deposition method and a minimum 90 nm^2 atomically flat surface by electron beam deposition with roughness values smaller than 0.200 nm. However, regarding the films deposited by electron beam deposition, we faced with reproducibility problem based on a problem about electrical connections of the evaporator. In brief, these two films have macroscopic homogeneity and mechanical stability enough to study with quartz crystal microbalance. Only remaining requirement is the special care for the attachment of electrical connectors to the electrode surfaces since there are not any adhesive layer. As for the helium atom diffraction study, these two films have a comparable surface morphology with the gold film produced in the study of Danışman has [30]. Then, we have concluded that they are suitable to study with helium atom diffraction.

REFERENCES

[1] Buchhloz, S., Fuchs, H., Rabe, J. P., *J. Vac. Sci. Technol., B*, 1991, 9, 857

[2] Golan, Y., Margulis, L., Rubinstein, I., *Surf. Sci.*, 1992, 264, 312

[3] Chidsey, C. E. D., Loiacono, D. N., Sleator, T., Nakahara, S., *Surf. Sci.*, 1988, 200, 45

[4] Guo, L. H., Facci, J. S., McLendon, G., Mosher, R., *Langmuir*, 1994, 10, 4588

[5] Putman, A., Blackford, B. L., Jericho, M. H., Watanbe, M. O., *Surf. Sci.*, 1989, 217, 276

[6] Watanabe, M. O., Kuroda, T., Tanaka, K., Sakai, A., *J. Vac. Sci. Technol., B*, 1991, 9, 924

[7] Vancea, J., Reiss, G., Schneider, F., Bauer, K., Hoffmann, H., *Surf. Sci.*, 1989, 218, 108

[8] Porath, D., Goldstein, Y., Grayevsky, A., Millo, O., *Surf. Sci.*, 1994, 321, 81

[9] DeRose, J. A. Thundat, T., Nagahara, L. A., Lindsay, S. M., *Surf. Sci.*, 1991, 256, 102

[10] Bottomley, L. A., Coury, J. E., First, P. N., *Anal. Chem.*, 1996, 68, R185

[11] Poirier, G. E., *Langmuir,* 1999, 15, 1167.

[12] Dhirani, A., Hines, M. A., Fisher, A. J., Ismail, O., Guyotsionnest, P., *Langmuir*, 1995, 11, 2609.

[13] Ulman, A., *Chem. Rev.*, 1996, 96, 1533

[14] Klein,H.,Blanc, W.,Pierrisnard, R.,Fauquet, C.,Dumas Ph., *Eur. Phys. J. B*, 2000, 14, 371

[15] Love, J. C., Estroff, L. A., Kriebel, J. K., Nuzzo, R. G., Whitesides, G. M., *Chem. Rev.*, 2005, 105 (4), 1103

[16] Chaki, N. K., Vijayamohanan, K., *Biosens. Bioelectron.*, 2002, 17 (1-2), 1

[17] Kepley, L.J., Crooks, R.M., Ricco, A.J., *Anal. Chem.*, 1992, 64, 3191

[18] Bose, M.,Base, D.K., Bose, D. N., *Appl. Surf. Sci.*, 2001, 171, 130

[19] Buttry,D.A.,Ward, M.D., *Chem. Rev*., 1992, 92, 1355

[20] Gewirth,A.A., Niece,B.K., *Chem. Rev*., 1997, 97(4), 1129

[21] Nogues, C.,Wanunu, M., *Surf. Sci*., 2004, 573, L383

[22] Stamou, D., Gourdon, D., Liley, M., Burnham, N. A., Kulik, A., Vogel, H., Duschl, C., *Langmuir*, 1997, 13, 2425

[23] Semaltianos, N. G., Wilson, E. G., *Thin Solid Films*, 2000, 366, 111

[24] Hwang, J., Dubson, M. A., *J. Appl. Phys.*, 1992, 72, 1852

[25] Lauer, M .E., Jungmann, R., Kindt, J. H., Magonov, S., Fuhrhop, J. H., Oroudjev, E., Hansma, H. G., *Langmuir*, 2007, 23, 5459

[26] Dishner, M. H., Ivey, M. M., Gorer, S., Hemminger, J. C., *J. Vac. Sci. Technol*., A, 1998, 16(6), 3295

[27] Höphner, U., Hehl, H., Brehmer, L., *Appl. Surf. Sci*., 1999, 152, 259

[28] Wieckowski, A., *Interfacial Electrochemistry: Theory, Experiment and Applications*, 1999, Marcel Dekker, New York

[29] http://www.ecliptek.com/crystals/glossary.html, last access date: 26 July 2010

[30] Danışman, M. F., ''Surface Diffraction Studies of Organic Thin Films'', Doctor of Philosophy Thesis, Princeton University, Department of Chemistry, 2005

[31] Oura, K., Lifshits, V. G., Saranin, A. A., Zotov, A. V., Katayama, M., *Surface Science An Introduction*, 2003, Springer, Berlin

[32] Kittel, C., *Introduction to Solid State Physics*, 1971, Wiley, New York

[33] Harsha, K. S. S., *Principles of Vapor Deposition of Thin Films*, 2005, Elsevier, Amsterdam

[34] Huang, Y., Qiu, H., Wang, F., Pan, L., Tian, Y., Wu, P., *Vacuum*, 2003, 71, 523

[35] Lee, D., et al., Surface Science,2009,603,2978

[36] Liu, H. Z., Brown, N. M. D., Mckinley, A., *J. Phys. Condens. Matter*, 1997, 9, 59

[37] Higo, M., Fujita, K., Tanaka, Y., Mitsushio,M., Yoshidome, T., *Appl. Surf. Sci.*, 2006, 252, 5083

[38] Levlin, M., Laakso, A., Niemi, H. E. M., Hautojarvi, P., *Appl. Surf. Sci.*,1997, 115,31

[39] Şahin, D., ''Structural and Electrical Properties of Flash Memory Cells With HfO_2 Tunnel Oxide and With/Without Nanocrystals'', Master of Science Thesis, Middle East Technical University, Graduate School of Natural and Applied Sciences, Department of Physics, 2009

[40] Çolakoğlu, T., ''The Effects of Post-Annealing Process On The Physical Properties of Silver-Indium-Selenium Ternary Semiconductor Thin Films Deposited by Electron Beam Technique'', Doctor of Philosophy Thesis, Middle East Technical University, Graduate School of Natural and Applied Sciences, Department of Physics, 2009

[41] Digital Instruments Veeco Metrology Group, *Multimode™ SPM Instruction Manual*, Version 4.31ce, 1997

[42] Daniels, S. L., Ngunjiri, J. N., Garno, J. C., *Anal. Bioanal. Chem*., 2009, 394, 215-223

[43] http://web.mit.edu./cortiz/www/afm.gif, last access date: 7 July 2010

[44] Digital Instruments Veeco Metrology Group, *Command Reference Manual*, Version 5.12 r3, 2002